terol (19) and SM (53). We further characterized the role of lipid on the plasma membrane in viral infectivity and found that cholesterol depletion by B-CD, as well as hydrolysis of SM by SMase, moderately inhibits HCV infectivity (Fig. 5). These results suggest that cholesterol and sphingolipid in the plasma membrane environment may assist HCV entry, while HCV virion-associated cholesterol and sphingolipid appear to play critical roles in viral infection.

We previously demonstrated that HCV RNA and nonstructural proteins are present in DRM structures, likely in the context of a lipid-raft structure, and that viral RNA is likely synthesized at a raft membrane structure in cells containing the genotype 1b HCV replicon (2, 10, 46). Here we observed that ISP-1 and HPA-12 suppress HCVcc production, but not viral RNA replication, by the JFH-1 replicon (Fig. 6). Impairment of particle assembly and maturation, rather than suppression of genome replication, by these drugs may account for the inhibition of HCV production in the JFH-1 system. Viral RNA replication of the HCV-N replicon, however, was efficiently inhibited by these compounds, as found in previous reports (43). The virus strain specificity of the anti-HCV activity of cyclosporine has recently been demonstrated: JFH-1 replication is less sensitive to cyclosporine than replication of genotype 1b strains. Furthermore, the requirement for interaction with a cellular replication cofactor, cyclophilin B, differs among HCV strains (18). It appears that ISP-1 and HPA-12 are further examples of diverse effects on HCV strain replication.

In summary, our data here demonstrate important roles of cholesterol and sphingolipid in HCV infection and virion maturation. Specifically, mature HCV particles are rich in cholesterol. Depletion from HCV or hydrolysis of virion-associated SM results in a loss of infectivity. Moreover, the addition of exogenous cholesterol restores infectivity. In addition, cholesterol and sphingolipid on the HCV membrane play key roles in virus internalization, and portions of structural proteins are localized at lipid-raft-like membrane structures within cells. Finally, inhibitors of the sphingolipid biosynthetic pathway efficiently block virion production. These observations suggest that agents capable of modifying virion-associated lipid content might function as antivirals by preventing and/or blocking HCV infection and production.

ACKNOWLEDGMENTS

We thank M. Matsuda, M. Sasaki, S. Yoshizaki, T. Shimoji, M. Kaga, and T. Date for technical assistance and T. Mizoguchi for secretarial work.

This work was partially supported by a grant-in-aid for Scientific Research from the Japan Society for the Promotion of Science, from the Ministry of Health, Labor, and Welfare of Japan, and from the Ministry of Education, Culture, Sports, Science, and Technology, as well as by a Research on Health Science Focusing on Drug Innovation grant from the Japan Health Sciences Foundation.

REFERENCES

1. **Aizaki, H., Y. Aoki, T. Harada, K. Ishii, T. Suzuki, S. Nagamori, G. Toda, Y. Matsuura, and T. Miyamura.** 1998. Full-length complementary DNA of hepatitis C virus genome from an infectious blood sample. Hepatology **27:** 621–627.
2. **Aizaki, H., K. J. Lee, V. M. Sung, H. Ishiko, and M. M. Lai.** 2004. Characterization of the hepatitis C virus RNA replication complex associated with lipid rafts. Virology **324:**450–461.
3. **Akazawa, D., T. Date, K. Morikawa, A. Murayama, M. Miyamoto, M. Kaga, H. Barth, T. F. Baumert, J. Dubuisson, and T. Wakita.** 2007. CD81 expression is important for the permissiveness of Huh7 cell clones for heterogeneous hepatitis C virus infection. J. Virol. **81:**5036–5045.
4. **Bender, F. C., J. C. Whitbeck, H. Lou, G. H. Cohen, and R. J. Eisenberg.** 2005. Herpes simplex virus glycoprotein B binds to cell surfaces independently of heparan sulfate and blocks virus entry. J. Virol. **79:**11588–11597.
5. **Blanchard, E., D. Brand, S. Trassard, A. Goudeau, and P. Roingeard.** 2002. Hepatitis C virus-like particle morphogenesis. J. Virol. **76:**4073–4079.
6. **Chazal, N., and D. Gerlier.** 2003. Virus entry, assembly, budding, and membrane rafts. Microbiol. Mol. Biol. Rev. **67:**226–237.
7. **Evans, M. J., T. von Hahn, D. M. Tscherne, A. J. Syder, M. Panis, B. Wolk, T. Hatziioannou, J. A. McKeating, P. D. Bieniasz, and C. M. Rice.** 2007. Claudin-1 is a hepatitis C virus co-receptor required for a late step in entry. Nature **446:**801–805.
8. **Ezelle, H. J., D. Markovic, and G. N. Barber.** 2002. Generation of hepatitis C virus-like particles by use of a recombinant vesicular stomatitis virus vector. J. Virol. **76:**12325–12334.
9. **Fukasawa, M., M. Nishijima, H. Itabe, T. Takano, and K. Hanada.** 2000. Reduction of sphingomyelin level without accumulation of ceramide in Chinese hamster ovary cells affects detergent-resistant membrane domains and enhances cellular cholesterol efflux to methyl-β-cyclodextrin. J. Biol. Chem. **275:**34028–34034.
10. **Gao, L., H. Aizaki, J. W. He, and M. M. Lai.** 2004. Interactions between viral nonstructural proteins and host protein hVAP-33 mediate the formation of hepatitis C virus RNA replication complex on lipid raft. J. Virol. **78:**3480–3488.
11. **Guo, J. T., V. V. Bichko, and C. Seeger.** 2001. Effect of alpha interferon on the hepatitis C virus replicon. J. Virol. **75:**8516–8523.
12. **Hanada, K., T. Hara, M. Fukasawa, A. Yamaji, M. Umeda, and M. Nishijima.** 1998. Mammalian cell mutants resistant to a sphingomyelin-directed cytolysin. Genetic and biochemical evidence for complex formation of the LCB1 protein with the LCB2 protein for serine palmitoyltransferase. J. Biol. Chem. **273:**33787–33794.
13. **Hase, T., P. L. Summers, K. H. Eckels, and W. B. Baze.** 1987. An electron and immunoelectron microscopic study of dengue-2 virus infection of cultured mosquito cells: maturation events. Arch. Virol. **92:**273–291.
14. **Heider, J. G., and R. L. Boyett.** 1978. The picomole determination of free and total cholesterol in cells in culture. J. Lipid Res. **19:**514–518.
15. **Heinz, F. X., and S. L. Allison.** 2003. Flavivirus structure and membrane fusion. Adv. Virus Res. **59:**63–97.
16. **Huang, H., F. Sun, D. M. Owen, W. Li, Y. Chen, M. Gale, and J. Ye.** 2007. Hepatitis C virus production by human hepatocytes dependent on assembly and secretion of very low-density lipoproteins. Proc. Natl. Acad. Sci. USA **104:**5848–5853.
17. **Ikeda, M., M. Yi, K. Li, and S. M. Lemon.** 2002. Selectable subgenomic and genome-length dicistronic RNAs derived from an infectious molecular clone of the HCV-N strain of hepatitis C virus replicate efficiently in cultured Huh7 cells. J. Virol. **76:**2997–3006.
18. **Ishii, N., K. Watashi, T. Hishiki, K. Goto, D. Inoue, M. Hijikata, T. Wakita, N. Kato, and K. Shimotohno.** 2006. Diverse effects of cyclosporine on hepatitis C virus strain replication. J. Virol. **80:**4510–4520.
19. **Kapadia, S. B., H. Barth, T. Baumert, J. A. McKeating, and F. V. Chisari.** 2007. Initiation of hepatitis C virus infection is dependent on cholesterol and cooperativity between CD81 and scavenger receptor B type I. J. Virol. **81:**374–383.
20. **Kato, T., A. Furusaka, M. Miyamoto, T. Date, K. Yasui, J. Hiramoto, K. Nagayama, T. Tanaka, and T. Wakita.** 2001. Sequence analysis of hepatitis C virus isolated from a fulminant hepatitis patient. J. Med. Virol. **64:**334–339.
21. **Kato, T., T. Date, M. Miyamoto, A. Furusaka, K. Tokushige, M. Mizokami, and T. Wakita.** 2003. Efficient replication of the genotype 2a hepatitis C virus subgenomic replicon. Gastroenterology **125:**1808–1817.
22. **Kato, T., T. Date, M. Miyamoto, M. Sugiyama, Y. Tanaka, E. Orito, T. Ohno, K. Sugihara, I. Hasegawa, K. Fujiwara, K. Ito, A. Ozasa, M. Mizokami, and T. Wakita.** 2005. Detection of anti-hepatitis C virus effects of interferon and ribavirin by a sensitive replicon system. J. Clin. Microbiol. **43:**5679–5684.
23. **Kato, T., T. Date, A. Murayama, K. Morikawa, D. Akazawa, and T. Wakita.** 2006. Cell culture and infection system for hepatitis C virus. Nat. Protoc. **1:**2334–2339.
24. **Kobayashi. S, K. Kakumoto, and M. Sugiura.** 2002. Transition metal salts-catalyzed aza-Michael reactions of enones with carbamates. Org. Lett. **18:** 1319–1322.
25. **Koutsoudakis, G., E. Herrmann, S. Kallis, R. Bartenschlager, and T. Pietschmann.** 2007. The level of CD81 cell surface expression is a key determinant for productive entry of hepatitis C virus into host cells. J. Virol. **81:**588–598.
26. **Lohmann, V., F. Korner, J. Koch, U. Herian, L. Theilmann, and R. Bartenschlager.** 1999. Replication of subgenomic hepatitis C virus RNAs in a hepatoma cell line. Science **285:**110–113.
27. **Mackenzie, J. M., and E. G. Westaway.** 2001. Assembly and maturation of the flavivirus Kunjin virus appear to occur in the rough endoplasmic reticulum and along the secretory pathway, respectively. J. Virol. **75:**10787–10799.
28. **Manes, S., G. del Real, R. A. Lacalle, P. Lucas, C. Gomez-Mouton, S. Sanchez-Palomino, R. Delgado, J. Alcami, E. Mira, and A. C. Martinez.**

2000. Membrane raft microdomains mediate lateral assemblies required for HIV-1 infection. EMBO 1:190–196.
29. **Matsuo, E., H. Tani, C. Lim, Y. Komoda, T. Okamoto, H. Miyamoto, K. Moriishi, S. Yagi, A. H. Patel, T. Miyamura, and Y. Matsuura.** 2006. Characterization of HCV-like particles produced in a human hepatoma cell line by a recombinant baculovirus. Biochem. Biophys. Res. Commun. **340:**200–208.
30. **Matto, M., C. M. Rice, B. Aroeti, and J. S. Glenn.** 2004. Hepatitis C virus core protein associates with detergent-resistant membranes distinct from classical plasma membrane rafts. J. Virol. **78:**12047–12053.
31. **Miyake, Y., Y. Kozutsumi, S. Nakamura, T. Fujita, and T. Kawasaki.** 1995. Serine palmitoyltransferase is the primary target of a sphingosine-like immunosuppressant, ISP-1/myriocin. Biochem. Biophys. Res. Commun. **211:** 396–403.
32. **Miyanari, Y., K. Atsuzawa, N. Usuda, K. Watashi, T. Hishiki, M. Zayas, R. Bartenschlager, T. Wakita, M. Hijikata, and K. Shimotohno.** 2007. The lipid droplet is an important organelle for hepatitis C virus production. Nat. Cell Biol. **9:**1089–1097.
33. **Morikawa, K., Z. Zhao, T. Date, M. Miyamoto, A. Murayama, D. Akazawa, J. Tanabe, S. Sone, and T. Wakita.** 2007. The roles of CD81 and glycosaminoglycans in the adsorption and uptake of infectious HCV particles. J. Med. Virol. **79:**714–723.
34. **Murakami, K., K. Ishii, Y. Ishihara, S. Yoshizaki, K. Tanaka, Y. Gotoh, H. Aizaki, M. Kohara, H. Yoshioka, Y. Mori, N. Manabe, I. Shoji, T. Sata, R. Bartenschlager, Y. Matsuura, T. Miyamura, and T. Suzuki.** 2006. Production of infectious hepatitis C virus particles in three-dimensional cultures of the cell line carrying the genome-length dicistronic viral RNA of genotype 1b. Virology **351:**381–392.
35. **Nakai, K., T. Okamoto, T. Kimura-Someya, K. Ishii, C. K. Lim, H. Tani, E. Matsuo, T. Abe, Y. Mori, T. Suzuki, T. Miyamura, J. H. Nunberg, K. Moriishi, and Y. Matsuura.** 2006. Oligomerization of hepatitis C virus core protein is crucial for interaction with the cytoplasmic domain of E1 envelope protein. J. Virol. **80:**11265–11273.
36. **Ng, M. L., J. Howe, V. Sreenivasan, and J. J. Mulders.** 1994. Flavivirus West Nile (Sarafend) egress at the plasma membrane. Arch. Virol. **137:**303–313.
37. **Ng, M. L., S. H. Tan, and J. J. Chu.** 2001. Transport and budding at two distinct sites of visible nucleocapsids of West Nile (Sarafend) virus. J. Med. Virol. **65:**758–764.
38. **Niwa, H., K. Yamamura, and J. Miyazaki.** 1991. Efficient selection for high-expression transfectants with a novel eukaryotic vector. Gene **108:**193–199.
39. **Pessin, J. E., and M. Glaser.** 1980. Budding of Rous sarcoma virus and vesicular stomatitis virus from localized lipid regions in the plasma membrane of chicken embryo fibroblasts. J. Biol. Chem. **255:**9044–9050.
40. **Pitha, J., T. Irie, P. B. Sklar, and J. S. Nye.** 1988. Drug solubilizers to aid pharmacologists: amorphous cyclodextrin derivatives. Life Sci. **43:**493–502.
41. **Rahman, S., T. Matsumura, K. Masuda, K. Kanemura, and T. Fukunaga.** 1998. Maturation site of dengue type 2 virus in cultured mosquito C6/36 cells and Vero cells. Kobe J. Med. Sci. **44:**65–79.
42. **Rouser, G., G. Galli, and G. Kritchevsky.** 1967. Lipid composition of the normal human brain and its variations during various diseases. Pathol. Biol. **15:**195–200.
43. **Sakamoto, H., K. Okamoto, M. Aoki, H. Kato, A. Katsume, A. Ohta, T. Tsukuda, N. Shimma, Y. Aoki, M. Arisawa, M. Kohara, and M. Sudoh.** 2005. Host sphingolipid biosynthesis as a target for hepatitis C virus therapy. Nat. Chem. Biol. **1:**333–337.
44. **Sato, K., H. Okamoto, S. Aihara, Y. Hoshi, T. Tanaka, and S. Mishiro.** 1993. Demonstration of sugar moiety on the surface of hepatitis C virions recovered from the circulation of infected humans. Virology **196:**354–357.
45. **Serafino, A., M. B. Valli, F. Andreola, A. Crema, G. Ravagnan, L. Bertolini, and G. Carloni.** 2003. Suggested role of the Golgi apparatus and endoplasmic reticulum for crucial sites of hepatitis C virus replication in human lymphoblastoid cells infected in vitro. J. Med. Virol. **70:**31–41.
46. **Shi, S. T., K. J. Lee, H. Aizaki, S. B. Hwang, and M. M. Lai.** 2003. Hepatitis C virus RNA replication occurs on a detergent-resistant membrane that cofractionates with caveolin-2. J. Virol. **77:**4160–4168.
47. **Shinitzky, M., and M. Inbar.** 1976. Microviscosity parameters and protein mobility in biological membranes. Biochim. Biophys. Acta **433:**133–149.
48. **Shirakura, M., K. Murakami, T. Ichimura, R. Suzuki, T. Shimoji, K. Fukuda, K. Abe, S. Sato, M. Fukasawa, Y. Yamakawa, M. Nishijima, K. Moriishi, Y. Matsuura, T. Wakita, T. Suzuki, P. M. Howley, T. Miyamura, and I. Shoji.** 2007. E6AP ubiquitin ligase mediates ubiquitylation and degradation of hepatitis C virus core protein. J. Virol. **81:**1174–1185.
49. **Stuart, A. D., H. E. Eustace, T. A. McKee, and T. D. Brown.** 2002. A novel cell entry pathway for a DAF-using human enterovirus is dependent on lipid rafts. J. Virol. **76:**9307–9322.
50. **Takikawa, S., K. Ishii, H. Aizaki, T. Suzuki, H. Asakura, Y. Matsuura, and T. Miyamura.** 2000. Cell fusion activity of hepatitis C virus envelope proteins. J. Virol. **74:**5066–5074.
51. **Tani, H., Y. Komoda, E. Matsuo, K. Suzuki, I. Hamamoto, T. Yamashita, K. Moriishi, K. Fujiyama, T. Kanto, N. Hayashi, A. Owsianka, A. H. Patel, M. A. Whitt, and Y. Matsuura.** 2007. Replication-competent recombinant vesicular stomatitis virus encoding hepatitis C virus envelope proteins. J. Virol. **81:**8601–8612.
52. **Umehara, T., M. Sudoh, F. Yasui, C. Matsuda, Y. Hayashi, K. Chayama, and M. Kohara.** 2006. Serine palmitoyltransferase inhibitor suppresses HCV replication in a mouse model. Biochem. Biophys. Res. Commun. **346:**67–73.
53. **Voisset, C., M. Lavie, F. Helle, A. Op De Beeck, A. Bilheu, J. Bertrand-Michel, F. Tercé, L. Cocquerel, C. Wychowski, N. Vu-Dac, and J. Dubuisson.** 2008. Ceramide enrichment of the plasma membrane induces CD81 internalization and inhibits hepatitis C virus entry. Cell. Microbiol. **10:**606–617.
54. **Wakita, T., T. Pietschmann, T. Kato, T. Date, M. Miyamoto, Z. Zhao, K. Murthy, A. Habermann, H. G. Krausslich, M. Mizokami, R. Bartenschlager, and T. J. Liang.** 2005. Production of infectious hepatitis C virus in tissue culture from a cloned viral genome. Nat. Med. **11:**791–796.
55. **Yasuda, S., H. Kitagawa, M. Ueno, H. Ishitani, M. Fukasawa, M. Nishijima, S. Kobayashi, and K. Hanada.** 2001. A novel inhibitor of ceramide trafficking from the endoplasmic reticulum to the site of sphingomyelin synthesis. J. Biol. Chem. **276:**43994–44002.
56. **Zhong, J., P. Gastaminza, G. Cheng, S. Kapadia, T. Kato, D. R. Burton, S. F. Wieland, S. L. Uprichard, T. Wakita, and F. V. Chisari.** 2005. Robust hepatitis C virus infection in vitro. Proc. Natl. Acad. Sci. USA **102:**9294–9299.

Available online at www.sciencedirect.com
ScienceDirect
Journal of Virological Methods 148 (2008) 174–181
Journal of Virological Methods
www.elsevier.com/locate/jviromet

Dynamic behavior of hepatitis C virus quasispecies in a long-term culture of the three-dimensional radial-flow bioreactor system

Kyoko Murakami [a], Yasushi Inoue [a,b], Su-Su Hmwe [a,c], Kazuhiko Omata [a,d], Tomokatsu Hongo [e], Koji Ishii [a], Sayaka Yoshizaki [a], Hideki Aizaki [a], Tomokazu Matsuura [f], Ikuo Shoji [a], Tatsuo Miyamura [a], Tetsuro Suzuki [a,*]

[a] *Department of Virology II, National Institute of Infectious Diseases, 1-23-1 Toyama, Shinjuku-ku, Tokyo 162-8640, Japan*
[b] *Pulmonary and Critical Care Unit, Mita Hospital, International University of Health and Welfare, Japan*
[c] *Department of Infectious Diseases, Internal Medicine, Graduate School of Medicine, University of Tokyo, Tokyo, Japan*
[d] *Department of Oral and Maxillofacial Surgery, The Nippon Dental University School of Dentistry at Tokyo, Tokyo, Japan*
[e] *ABLE Corporation, Shizuoka, Japan*
[f] *Department of Laboratory medicine, The Jikei University School of Medicine, Tokyo, Japan*

Received 25 July 2007; received in revised form 9 November 2007; accepted 21 November 2007

Abstract

Hepatitis C virus (HCV) exists in infected individuals as quasispecies, usually consisting of a dominant viral isolate and a variable mixture of related, yet genetically distinct, variants. A prior HCV infection system was developed using human hepatocellular carcinoma cells cultured in the three-dimensional radial-flow bioreactor (RFB), in which the cells retain morphological appearance and their differentiated hepatocyte functions for an extended period of time. This report studies the selection and alteration of the viral quasispecies in the RFB system inoculated with pooled serum derived from HCV carriers. Monitoring the viral RNA and core protein in the culture supernatants, together with nucleotide sequencing of hypervariable region 1 of the HCV genome, demonstrated that (1) the virus production intermittently fluctuated in the cultures, (2) the viral genetic diversity was markedly reduced 3 days post-infection (p.i.), and (3) dominant species changed on days 19–33 p.i., suggesting that the virus populations can be selected according to susceptibility to the viral infection and replication. A therapeutic effect of interferon-α also demonstrated the inhibition of HCV expression. Thus, this HCV infection model in the RFB system should be useful for investigating the dynamic behavior of HCV quasispecies in cultured cells and evaluating anti-HCV compounds.

Keywords: Hepatitis C virus; Three-dimensional culture; Radial-flow bioreactor; Dynamics; Quasispecies

1. Introduction

Hepatitis C virus (HCV) is a major cause of chronic liver diseases (Choo et al., 1989; Kuo et al., 1989; Saito et al., 1990) and has been estimated to infect more than 170 million people throughout the world (Poynard et al., 2003). Symptoms of persistent HCV infection extend from chronic hepatitis to cirrhosis and ultimately hepatocellular carcinoma (Choo et al., 1989; Kuo et al., 1989; Saito et al., 1990). HCV belongs to the genus *Hepacivirus*, included in the family of Flaviviridae, and possesses a viral genome of a single, positive-stranded RNA with a nucleotide (nt) length of approximately 9.6 kb (Choo et al., 1991; Grakoui et al., 1993; Hijikata et al., 1991). It has been shown that HCV, like many other RNA viruses, circulates within infected individuals as a diverse population and closely related variants are referred to as quasispecies (Martell et al., 1992). This quasispecies model of mixed virus populations may imply a significant survival advantage because the simultaneous presence of multiple variant genomes and/or high rate of generation of new variants allow rapid selection of the mutants are better suited to new environmental conditions (Pawlotsky, 2006).

Studies on HCV replication and development of selective antiviral drugs have been hampered primarily by the lack of efficient cell culture systems. Establishment of selectable dicistronic HCV RNAs that are capable of autonomous replication to high levels in human hepatoma Huh-7 cells was a

* Corresponding author. Tel.: +81 3 5285 1111; fax: +81 3 5285 1161.
E-mail address: tesuzuki@nih.go.jp (T. Suzuki).

0166-0934/$ – see front matter © 2007 Elsevier B.V. All rights reserved.
doi:10.1016/j.jviromet.2007.11.001

significant breakthrough in HCV research; however, virus production has not been observed in the conventional monolayer cultures (Blight et al., 2000; Lohmann et al., 1999). Recently, it has been described that infectious HCV particles are efficiently produced from a genotype 2a isolate JFH-1 in Huh-7 cells (Blight et al., 2000; Wakita et al., 2005; Zhong et al., 2005). This JFH-1 based HCV culture system is an invaluable achievement permitting a variety of studies on the complete HCV life cycle. However, HCV infection systems with human sera or plasmas containing intact virions are still limited because of low levels of propagation in the cultures. Reverse transcription (RT)-PCR was typically used to detect the viral RNA in cell extracts; however, synthesized viral proteins were not observed in these systems (Ikeda et al., 1998; Tagawa et al., 1995).

There are reports of differentiated human hepatoma FLC4 (functional liver cell 4) cells grown in a three-dimensional (3D) radial-flow bioreactor (RFB) that can be infected by HCV-positive serum and support viral replication (Aizaki et al., 2003). Furthermore, production and release of infectious HCV has been observed in the RFB system following transfection of FLC4 cells with *in vitro* transcribed HCV genomic RNA, as well as in a 3D system using Huh-7 cells harboring genome-length dicistronic RNAs (Murakami et al., 2006). The RFB system, in which the bioreactor column consists of a cylindrical matrix with porous bead microcarriers extended vertically, was aimed initially at developing artificial liver tissues and allows liver-derived cells to maintain morphological appearance as well as their physiological functions, such as the ability to synthesize albumin and drug-metabolizing activity mediated by cytochrome P450 (Iwahori et al., 2003). The radial-flow configuration permits full contact between culture medium and cells at a physiologic perfusion flow rate, and prevents excessive shear stresses and buildup of waste products, thus ensuring the long-term viability of 3D cell culture.

The aim of the present study was to characterize HCV dynamics in the RFB system during long-term cultures inoculated with pooled serum obtained from HCV carriers, and to examine the therapeutic effects of interferon-alpha (IFN-α) in this HCV infection model.

2. Materials and methods

2.1. Cell cultures

FLC4 cells (Aoki et al., 1998), which were derived from human hepatocellular carcinoma cells and negative for HCV RNA and HBV DNA, were maintained in serum-free ASF104 medium (Ajinomoto, Japan) supplemented with 4 g/L D-glucose on the collagen-coated dishes before inoculating into the RFB column. The RFB system (ABLE, Japan) was manipulated as described previously (Aizaki et al., 2003) with minor modifications. Briefly, RFB columns, which have bed volumes of 30 or 4 mL and are filled with porous glass microcarriers (diameter 0.6 mm, vacant capacity 50%, pore size <120 μm) (Hongo et al., 2005), were seeded with FLC4 cells, which subsequently attached to the surface and inside of porous glass beads. ASF104 medium containing 2% fetal calf serum was added at a flow rate of 50 mL/day, and the culture condition was automatically controlled by monitoring temperature, pH value and oxygen levels in the vessel throughout the duration of the study.

2.2. Infection of HCV-positive sera

HCV antibody-positive sera used in this study were blood donor samples supplied by The Japanese Red Cross Center, Tokyo, Japan. HCV RNA loads in the sera were as follows: serum A, 2.4×10^6 copies/mL; serum B, 8.6×10^6 copies/mL; serum C, 5.9×10^6 copies/mL; serum D, 2.5×10^6 copies/mL; serum E, 1.0×10^7 copies/mL; serum F, 1.4×10^7 copies/mL (Table 1). In the first experiment (Fig. 3), aliquots of each serum containing 2×10^6 copies of HCV RNA were mixed and pooled serum sample with 1.2×10^7 copies was prepared as an inoculum. The pooled serum (2.5 mL) was added to the 3D cultured-FLC4 cells in the 30-mL RFB column, and the culture medium was changed after 12 h of incubation. At various times during the culture period, culture medium (50 mL) was collected to determine HCV RNA and the core protein. Collected culture media were passed through a 0.20-μm filter to remove the debris, and stored at −80 °C. In the second experiment to evaluate a therapeutic effect of anti-HCV drug (Fig. 4), 4-mL RFB columns were used. IFN-α (Sumiferon 300; Sumitomo Pharmaceuticals, Japan) was added to one of two columns at a final concentration of 100 IU/mL after the infection. Culture medium was periodically collected for determination of HCV RNA, the core protein and transaminases, and was replaced with the same volume of fresh medium with or without IFN-α.

2.3. Quantitation of HCV RNA and core protein

HCV RNA was extracted from 140 μL of each serum or culture medium using QIAamp Viral RNA Mini spin column (QIAGEN); RNA was eluted in 60 μL of water and stored at −80 °C. Real-time RT-PCR was performed using TaqMan EZ RT-PCR Core Reagents (PE Applied Biosystems), as described previously (Aizaki et al., 2003; Suzuki et al., 2005). The viral core antigen in the culture medium was quantified by immunoassay (Ortho HCV-Core ELISA Kit; Ortho-Clinical Diagnotics), according to the manufacturer's instruction (Murakami et al., 2006).

2.4. PCR amplification and nucleotide sequencing of HVR1 domain and its flanking region

Five microliters of RNA samples prepared as above were reverse transcribed using SuperScript II (Invitrogen) and a specific primer 5′-CATCCATGTGCAGCCGAACC-3′ (corresponding to nucleotides [nt] 2006–1987 of HCV NIHJ1) (Aizaki et al., 1998). For the nested PCR, a genotype-independent set of primers specific for hypervariable region 1 (HVR1). The first round of PCR was performed with the outer sense primer 5′-GCATGGCTTGGGATATGATG-3′ (nt 1291–1310) and with the reverse transcription primer described above as the outer antisense primer. After the initial 3.5-min denaturation step at 94 °C, 35 PCR cycles, with each cycle

Table 1
HCV-positive sera used in this study

Serum	Clone	HCV HVR1 sequence	% in the serum	genotype
A	A1	KVLIVMLSFAGVDGSTRTIGGRTAHTTQGSASLFSSGPAQKIQLINTNGS	75	1
	A2	-------L------N-H-V--AV-SS---FT---KL----------S---	12.5	
	A3	-------L------N-YAS---AGLL-R-V--I-TA----------S---	12.5	
B	B1	KVVVILLLAAGVDAGTNTIGGSAAQTTSGFTGLFRSGARQNIQLINTNGS	50	2
	B2	----------R	12.5	
	B3	----------S---------	12.5	
	B4	--L-V---F-----E-HVT--N-GR--A-LV--LTP--K----------	12.5	
	B5	--I----------	12.5	
C	C1	KVLIVMLLFAGVDGDTHVSGGTQGRAAYGLASLFALGPTQKIQLVNTNGS	83.3	1
	C2	----------A----------	16.7	
D	D1	KVLIVMLLFAGVDGVTHTSGAAAGHNARSLSGLFSLGSAQKLQLINTNGS	40	1
	D2	----------A-Y---GT--Y-TKTFT-F--R-PS--I--------	20	
	D3	----------T--Y---T-T----P--------V-----	10	
	D4	----------V---T----P--------V-----	10	
	D5	----------V-----	10	
	D6	----------Y-T--FT----S-----I--V-----	10	
E	E1	KVLIVMLLFAGVDGSTRVSGGQAGRVTKSLASFFSPGPQQKIQLVNSNGS	40	1
	E2	----------HGFT-L--A-S----------	30	
	E3	----------QGFT-L--A-S----------	10	
	E4	----------S-FT-L-TV----------	10	
	E5	----------N-Y---------AH--T-L--A-S----------	10	
F	F1	KVLIVMLLFAGVDGETNVMGGRAGHTTNTFTSLFSVGPAQKIQLVNSNGS	37	1
	F2	----------D-K----------S-L----N---S----------	27	
	F3	----------K----Q-----S-L----N---S----------	18	
	F4	----------A-------A--TK---------D----	9	
	F5	----------G--------A--A--L----TR--S----------	9	

consisting of 1 min at 94 °C, 2 min at 45 °C, and 3 min at 72 °C, were carried out, followed by a 10-min extension step at 72 °C. The second round was performed with the inner sense primer 5′-GGTAAGCTTTCCATGGTGGGGAACTGGGC-3′ (nt 1419–1447) and the inner antisense primer 5′-CTGGAATTCGCAGTCCTGTTGATGTGCCA-3′ (nt 1627–1599). The amplified products were cloned into the pGEM-T vector (Promega), and at least 8 independent clones were sequenced with an automatic DNA sequencer (ABI PRISM 310, PE Applied Biosystems).

3. Results

3.1. The outline of the RFB system

The RFB system was initially aimed at developing artificial liver tissues and allows liver-derived cells to maintain morphological appearance as well as their physiological functions, such as the ability to synthesize albumin and drug-metabolizing activity mediated by cytochrome P450 (Iwahori et al., 2003). Fig. 1 shows the outline of the RFB system. The bioreactor column consists of a vertically extended cylindrical matrix with porous glass microcarriers, which were most suitable for FLC4 culture as described in Section 2. The conditioning vessel is connected to a circulation system including tanks either for supplying fresh medium or for recovering sample aliquots. Oxygen consumption, temperature and pH of the culture medium are monitored continuously and conditioned in the vessel by computer and mass flow controller throughout the culture. Thus, the radial-flow configuration permits full contact between culture medium and cells at a physiologic perfusion flow rate, and prevents excessive shear stresses and a buildup of waste products, thus ensuring the long-term viability of 3D culture. For the long-term culture up to 110 days, temperature in the vessel gradually decreased from 37 to 30 °C as shown in Fig. 2A. The oxygen consumption, which indicates the cell growth condition, increased slowly from days 0 to 80 post-inoculation of the cells, and maintained a constant level afterwards. Under this condition, the production rate of albumin was found to be stable from days 15 to 105. The following experiments of HCV infection were done in such a stable phase of the cell condition after 3 weeks of pre-culture. Cell grown in the RFB column reached confluence at the end of culture (day 110) since the cells were observed outside the matrix bed (Fig. 2B).

3.2. Infection of HCV-positive sera to RFB cultured FLC4 cells

Previously, HCV RNA could be detected in FLC4 cells grown in the RFB up to 4 weeks of culture following inoculation with an HCV carrier plasmid (Aizaki et al., 2003). Establishment of a long-term stable culture system of human liver-derived cells

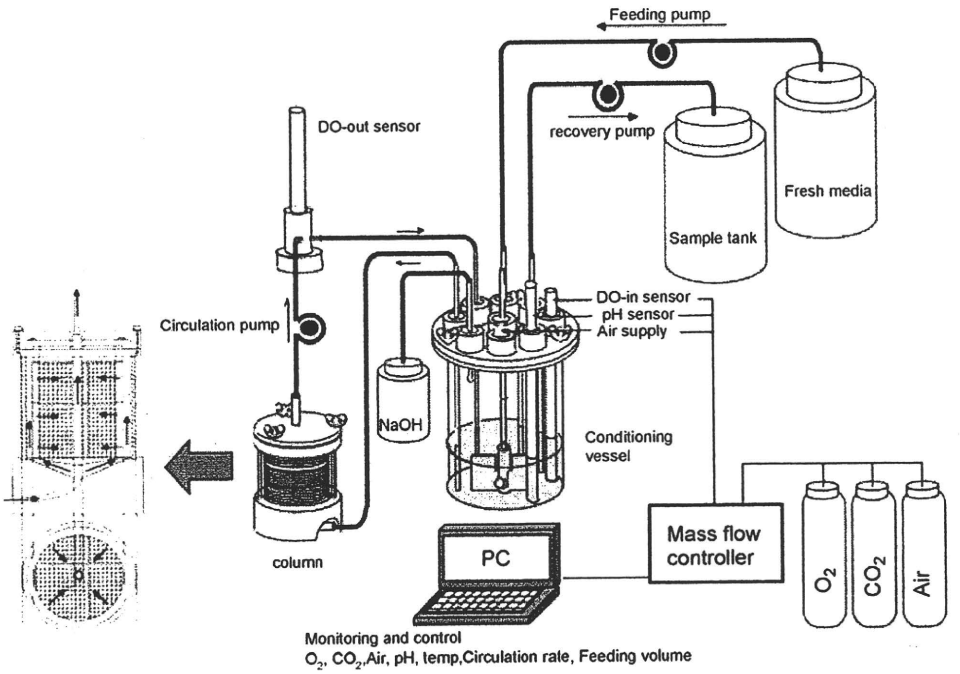

Fig. 1. Outline of the RFB system. RFB system consists of vessel, column and PC monitoring system. Culture condition was automatically controlled: oxgen concentration, temperature, pH, and oxgen level in the conditioning vessel are continuously monitored by PC and conditioned by mass flow controller.

retaining their differentiated hepatocyte function, as described above, enables evaluations of dynamic analysis of HCV replication and selection of viral variability and quasispecies. The potential of this culture system for screening HCV-positive sera was well suited for the viral infection.

Table 1 shows the serum samples (A–F) from six HCV carriers. The nucleotide complexity of HCV in serum samples was determined by sequencing the 1449–1598 nt region of the HCV genome, which includes HVR1 located at the N-terminal region of E2. Each serum was a mixture of a dominant HCV clone and related but distinct viral populations. The dominant species in sera A, C, D, E, and F were found to be genotype 1, and that in serum B was genotype 2. Viral loads in A–F, respectively, were 2.4×10^6, 8.6×10^6, 5.9×10^6, 2.5×10^6, 1.0×10^7 and 1.4×10^7 copies/mL, which were determined by real-time RT-PCR, as previously described (Aizaki et al., 2003; Suzuki et al., 2005). HCV loads of 2×10^6 copies from each serum sample were mixed to prepare a pooled serum sample containing 1.2×10^7 copies of HCV RNA. After FLC4 cells were inoculated into the RFB and subjected to 2 weeks of pre-culture for the preparation of 3D culture, the cells were infected with the pooled serum. Cell number at infection was about 10^8 in the 30-

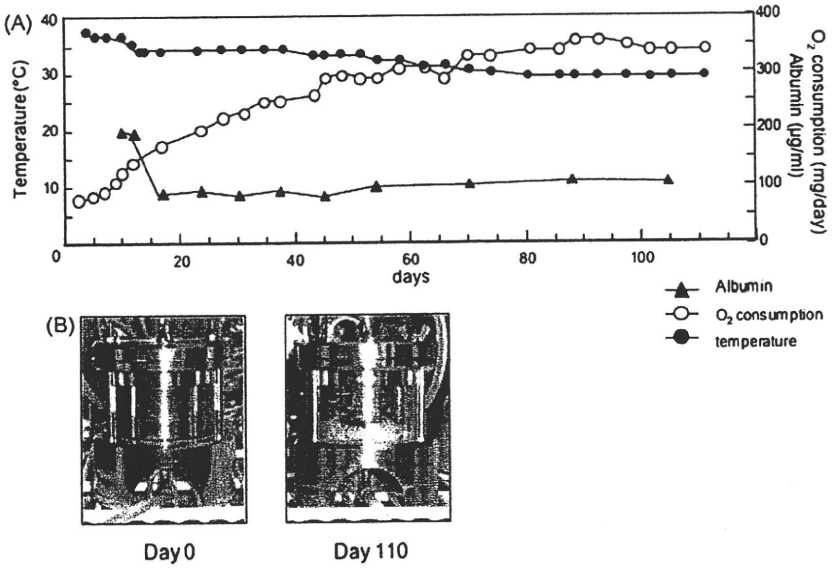

Fig. 2. Long-term culture of FLC4 cells in the RFB system. (A) Long-term culture of FLC4 cells in the RFB system. Temperature (closed circles) was gradually decreased from 37 to 30 °C. Oxygen consumption (open circles) was gradually increased from days 0 to 80 and reached the steady-state level. Albumin concentration (closed triangles) was constant from days 15 to 105. (B) The appearance of the RFB column at the beginning (day 0) and at the end (day 110) of culture.

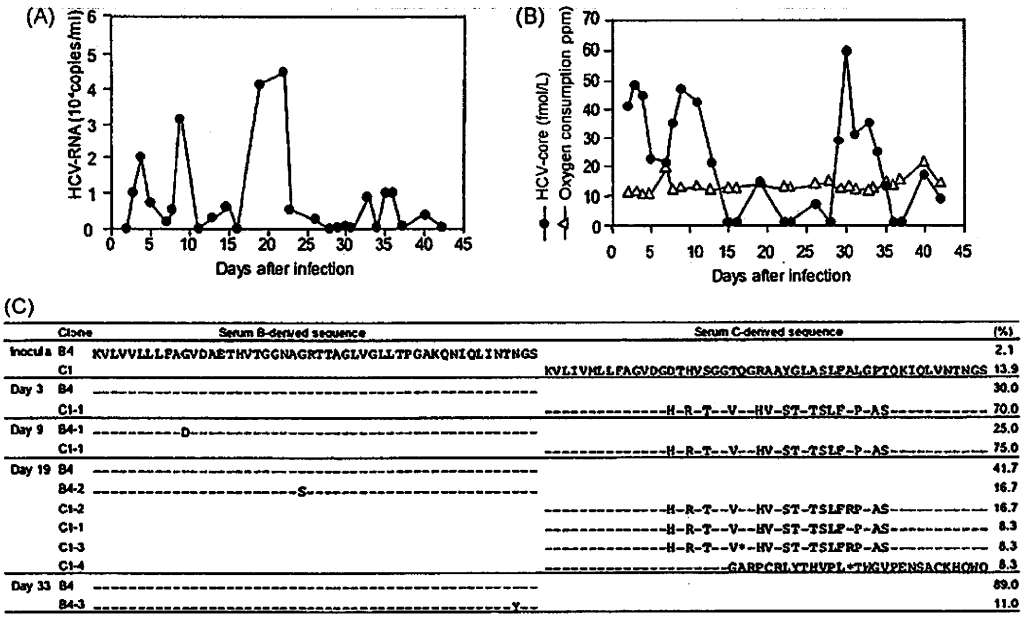

Fig. 3. HCV propagation in FLC4 cells cultured in the RFB system following inoculation with pooled sera obtained from HCV carriers. The 3D-cultured FLC4 cells were incubated with a pooled serum sample for 12 h, followed by changing the culture medium to fresh one. Culture medium was periodically collected for 42 days after inoculation, and HCV RNA and the viral core protein were quantified, respectively, by real-time RT-PCR and ELISA. (A) HCV RNA level in culture supernatant. (B) HCV-core protein (closed circles) and oxygen consumption (open triangles) levels in culture supernatant. (C) Changes in the viral quasispecies distribution after the inoculation. Percentages in the inoculum or in the culture medium at each time point (day 3, 9, 19, or 33 p.i.) are indicated at the right side. *, termination codon.

mL RFB column, as estimated from the glucose consumption (Kawada et al., 1998). Culture medium in the RFB was replaced with fresh medium 12 h post-infection (p.i.) and periodically sampled for 42 days.

Fig. 3A and B shows the levels of HCV RNA and viral core protein in the culture medium, respectively. HCV RNA was not observed on the first 2 days following infection, but was detectable from day 3 p.i. Viral RNA levels fluctuated, with peaks on days 3, 9, 19–21 and 33–36 p.i. At days 19–21 p.i., the average amount of HCV RNA detected in the culture supernatant was approximately 3×10^6 copies/day. Intermittent peaks were observed in HCV core protein levels in the culture supernatant, and the peak pattern of the core protein was largely consistent with that of viral RNA. During the infection experiment, the level of oxygen consumption was constant at approximately 12 ppm, thus suggesting that the desired conditions (constant or very gradually increasing cell number) were maintained.

3.3. Quasispecies analysis in RFB culture

The above results suggest that, although the environment was consistent in the pooled serum infection, there were periods in which the viruses actively replicated and released from the cells and periods in which they poorly replicated. The pooled serum used for the infection exhibited HCV populations had at least 26 distinct quasispecies (Table 1). To investigate whether the quasispecies distribution was altered due to infection, and whether HCV populations are selected during long-term culture in the RFB, total RNA was extracted from the culture supernatant samples collected on days 3, 9, 19 and 33 p.i., and the nucleotide sequence of the region containing HVR1 was determined, as described above. As shown in Fig. 3C, it is of interest that only two HCV species were detected in the sample at day 3 p.i.; the dominant clone C1-1, comprising approximately 70% of the viral population, and clone B4, comprising 30%. Although clone C1-1 was not detected in the sequence of the inoculum shown in Table 1, it was most similar to clone C1, a dominant clone in plasma C, among the HCV population observed in the inoculum; thus, it is possible that clone C1-1 is one of the minor species in serum C. Clone B4 was found to be derived from serum B. An almost identical HCV population was observed in the sample at day 9 p.i. In this sample, the dominant clone C1-1 and clone B4-1, which differs from clone B4 by only one amino acid, were detected. In contrast, more significant variation in quasispecies structure of the HCV species was observed in the sample at day 19 p.i. than that at day 9 p.i. With B4 as the dominant clone, the serum B-derived HCV species, clones B4 and B4-2, which differs from clone B4 by one amino acid, comprised 58% of the total population. Four types of HCV sequences derived from serum C were detected. Two of these (clones C1-3 and C1-4) contained lethal mutations. It was also found that the HCV species detected in the sample at day 33 p.i. included only two clones (clones B4 and B4-3), derived from serum B. The dominant clone, B4, was found to comprise 89% of the total population.

3.4. Potential use of the RFB system for evaluation of anti-HCV compounds

An experiment was carried out to determine whether this HCV infection experiment system was useful for the evaluation of anti-HCV drugs (Fig. 4). For this purpose, a small,

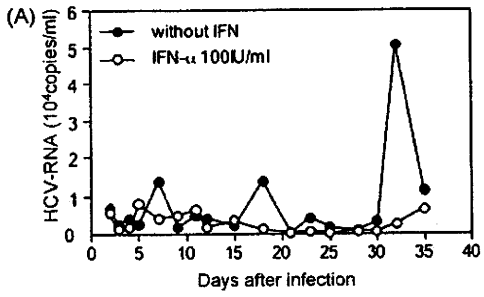

(B)

	Clone		(%)
Inocula	B4	K*LV*LLLFAGVDAETHVTGGNAGRTTAGLVGLLTPGAKQNIQLINTNGS	2.1
	C1	K*LIVMLLFAGVDGDTHVSGGTQGRAAYGLASLFALGPTQKIQLVNTNGS	13.9
Day 32	B4	----------	60
	B4-4	----------*----------	20
	C1-1	----------H-R-T--V--KV-ST-TSLF-P-AS----------	20

Fig. 4. A therapeutic effect of IFN in HCV infection model in the RFB cultures. HCV-infected FLC4 cells were treated with or without 100 IU/mL IFN-α. (A) Culture media were periodically collected, and HCV RNA levels were determined. Closed circles: without IFN treatment, open circles: treatment with IFN. (B) Changes in the viral quasispecies distribution in the cells without IFN treatment. Percentages in the inoculum or in the culture medium on day 32 p.i. are indicated at the right side. *, termination codon.

4-mL RFB column was adopted and a pair of RFB cultures infected with the HCV-positive pooled plasma (Table 1) was prepared. IFN-α was added to one culture at a final concentration of 100 IU/mL at 12 h p.i. No cytotoxicity was observed in FLC4 cells under these conditions (data not shown). Culture media from two cultures (12.5 mL each) were sampled periodically for 35 days and replaced by the same volume of fresh medium in the presence or absence of IFN-α. HCV RNA in the collected media was quantified by real-time RT-PCR, as described above. As shown in Fig. 4A, in the no-treatment culture, fluctuations in the viral RNA levels with the peaks on days 7, 18, and 32 p.i. ($1.5–5 \times 10^4$ copies/mL) were observed. However, while HCV RNA at $0.5–0.8 \times 10^4$ copies/mL was detected in the IFN-treated culture at days 5–11 p.i., no HCV RNA was detected at days 12–30 p.i. Serum levels of hepatic transaminases such as ALT and AST are known to be markers of liver damage. In the HCV-infection model with FLC4 cells cultured in RFB, the AST levels in the culture medium, which ranged from 5 to 10 IU/L without HCV infection, increased to 20–50 IU/L according to the viral infection (data not shown). Such increased AST levels were found to fall by the IFN treatment to lower than 10 IU/L at day 28 p.i. As reported previously, the ALT levels in the culture medium were constantly low; its levels were less than 10 IU/mL, with or without HCV infection (Aizaki et al., 2003). The viral nucleotide sequence in the no-treatment culture medium at day 32 p.i. was determined. It was found that serum B-derived clone B4 was dominant, and serum C-derived clone C1 was present as a minor clone (Fig. 4B); thus, the results corresponded well with those demonstrated in Fig. 3. An increase in viral RNA in the IFN-treated culture after day 32 p.i. was observed; although the degree of increase was only slight (Fig. 4A). It will be interesting to test whether HCV species grown in the IFN-treated culture is a variant resistant to IFN-α.

4. Discussion

At present an important limitation of the *in vitro* HCV infection system is that the only established culture system is based on genotype 2a, JFH-1 isolate, and Huh-7-derived cell lines. The development of alternate infection systems in which other HCV strains and host cells are available has been needed for the study of HCV dynamics and virus–host interactions, and for testing antivirals. This paper demonstrates that a long-term culture of the 3D RFB system is a useful tool for investigating HCV dynamics. The present results revealed that the viral quasispecies distribution altered in the HCV infection system in the RFB system. The change probably occurs in the following two-stage process. The first change was observed on day 3 p.i.; thus, it is possible that the HCV species were selected according to infectivity in FLC4 cells. It has been reported that HCV particle populations in chronic hepatitis C patients consist of low-density virions and higher-density immune complex forms (Hijikata et al., 1993; Kanto et al., 1994). Inoculation of cultured cells with HCV has demonstrated that the immune complex forms were less infective than the antibody-unbound virions (Shimizu et al., 1994). Therefore, another hypothesis may be that a large number of HCV populations in sera A, D, E, and F are immune complex forms; thus, these sera are less susceptible to the cells than sera B and C. The second change was observed on days 19–33 p.i. While the serum C-derived clone was dominant in the early stages after infection, the serum B-derived HCV clone became dominant over time. In the absence of immunological selection pressure, viral nucleotide mutations at random positions are accumulated during viral replication, and the newly generated variant species are selected principally, if not solely, based on the intrinsic replicative advantages or disadvantages that these mutations confer. Thus, these results suggest that the use of pooled serum sample allowed for screening of infectious materials compatible for the RFB culture.

Evaluation methods for anti-HCV drugs using monolayer culture systems with various culture cells, such as the replicon system and the JFH-1 based virion production system, have been reported (Bartenschlager et al., 2003; Blight et al., 2000; Boriskin et al., 2006; Lanford et al., 2003; Lindenbach et al., 2005; Lohmann et al., 1999; Wakita et al., 2005; Zhong et al., 2005). These methods utilize viral markers, such as HCV RNA and antigens, as indicators of treatment efficacy. However, the utility of long-term cell culture systems for anti-HCV drug evaluation based on infection with human sera is still limited. The use of a chimpanzee model, the only non-human host for HCV infection, is restricted due to several reasons such as problematic availability and ethical consideration. Given intensive efforts to reduce and replace animal testing in the course of development of new therapies worldwide, the RFB-based HCV infection model is a potential alternative to animal models such chimpanzee for assessing anti-HCV compounds. According to the studies with regards to mathematical modeling of HCV kinetics (Dahari et al., 2005; Dixit et al., 2004; Layden et al., 2003; Layden-Almer et al., 2006; Perelson et al., 2005), IFN therapy against HCV infection generally generates a biphasic decline in viral load; there is a rapid decrease in the serum HCV RNA level over the

first 1 day of treatment, followed by the second phase, which is slower than the first-phase viral decline. To date, there were no such observable viral kinetics in the IFN treatment under such experimental settings. Further detailed kinetic analyses of the use of varying doses of IFN and of very early time points to evaluate the antiviral effect are in progress.

In summary, by investigating the dynamics of HCV populations in the RFB culture system, it was demonstrated that HCV was intermittently detected in the culture supernatants of long-term culture, and that changes in viral quasispecies appear to be related to this fluctuation in the virus level. It was also shown that an HCV-infection model using the RFB system is useful for evaluating potential antivirals. Further investigation on the infection and growth of various HCV-positive sera is currently being conducted in order to obtain an adaptive clone with higher replication efficiency in this culture system.

Acknowledgements

The authors thank T. Wakita and S. Nagamori for helpful discussion and suggestions. We also thank M. Matsuda, T. Shimoji and M. Yahata for technical assistance, and T. Mizoguchi for secretarial work. This work was supported in part by a grant for Research on Health Sciences focusing on Drug Innovation from the Japan Health Sciences Foundation; by grants-in-aid from the Ministry of Health, Labor and Welfare; and by the program for Promotion of Fundamental Studies in Health Sciences of the National Institute of Biomedical Innovation, Japan.

References

Aizaki, H., Aoki, Y., Harada, T., Ishii, K., Suzuki, T., Nagamori, S., Toda, G., Matsuura, Y., Miyamura, T., 1998. Full-length complementary DNA of hepatitis C virus genome from an infectious blood sample. Hepatology 27, 621–627.

Aizaki, H., Nagamori, S., Matsuda, M., Kawakami, H., Hashimoto, O., Ishiko, H., Kawada, M., Matsuura, T., Hasumura, S., Matsuura, Y., Suzuki, T., Miyamura, T., 2003. Production and release of infectious hepatitis C virus from human liver cell cultures in the three-dimensional radial-flow bioreactor. Virology 314, 16–25.

Aoki, Y., Aizaki, H., Shimoike, T., Tani, H., Ishii, K., Saito, I., Matsuura, Y., Miyamura, T., 1998. A human liver cell line exhibits efficient translation of HCV RNAs produced by a recombinant adenovirus expressing T7 RNA polymerase. Virology 250, 140–150.

Bartenschlager, R., Kaul, A., Sparacio, S., 2003. Replication of the hepatitis C virus in cell culture. Antivir. Res. 60, 91–102.

Blight, K.J., Kolykhalov, A.A., Rice, C.M., 2000. Efficient initiation of HCV RNA replication in cell culture. Science 290, 1972–1974.

Boriskin, Y.S., Pecheur, E.I., Polyak, S.J., 2006. Arbidol: a broad-spectrum antiviral that inhibits acute and chronic HCV infection. Virol. J. 3, 56.

Choo, Q.L., Kuo, G., Weiner, A.J., Overby, L.R., Bradley, D.W., Houghton, M., 1989. Isolation of a cDNA clone derived from a blood-borne non-A, non-B viral hepatitis genome. Science 244, 359–362.

Choo, Q.L., Richman, K.H., Han, J.H., Berger, K., Lee, C., Dong, C., Gallegos, C., Coit, D., Medina-Selby, R., Barr, P.J., et al., 1991. Genetic organization and diversity of the hepatitis C virus. Proc. Natl. Acad. Sci. U.S.A. 88, 2451–2455.

Dahari, H., Major, M., Zhang, X., Mihalik, K., Rice, C.M., Perelson, A.S., Feinstone, S.M., Neumann, A.U., 2005. Mathematical modeling of primary hepatitis C infection: noncytolytic clearance and early blockage of virion production. Gastroenterology 128, 1056–1066.

Dixit, N.M., Layden-Almer, J.E., Layden, T.J., Perelson, A.S., 2004. Modelling how ribavirin improves interferon response rates in hepatitis C virus infection. Nature 432, 922–924.

Grakoui, A., McCourt, D.W., Wychowski, C., Feinstone, S.M., Rice, C.M., 1993. Characterization of the hepatitis C virus-encoded serine proteinase: determination of proteinase-dependent polyprotein cleavage sites. J. Virol. 67, 2832–2843.

Hijikata, M., Kato, N., Ootsuyama, Y., Nakagawa, M., Shimotohno, K., 1991. Gene mapping of the putative structural region of the hepatitis C virus genome by in vitro processing analysis. Proc. Natl. Acad. Sci. U.S.A. 88, 5547–5551.

Hijikata, M., Shimizu, Y.K., Kato, H., Iwamoto, A., Shih, J.W., Alter, H.J., Purcell, R.H., Yoshikura, H., 1993. Equilibrium centrifugation studies of hepatitis C virus: evidence for circulating immune complexes. J. Virol. 67, 1953–1958.

Hongo, T., Kajikawa, M., Ishida, S., Ozawa, S., Ohno, Y., Sawada, J., Umezawa, A., Ishikawa, Y., Kobayashi, T., Honda, H., 2005. Three-dimensional high-density culture of HepG2 cells in a 5-ml radial-flow bioreactor for construction of artificial liver. J. Biosci. Bioeng. 99, 237–244.

Ikeda, M., Sugiyama, K., Mizutani, T., Tanaka, T., Tanaka, K., Sekihara, H., Shimotohno, K., Kato, N., 1998. Human hepatocyte clonal cell lines that support persistent replication of hepatitis C virus. Virus Res. 56, 157–167.

Iwahori, T., Matsuura, T., Maehashi, H., Sugo, K., Saito, M., Hosokawa, M., Chiba, K., Masaki, T., Aizaki, H., Ohkawa, K., Suzuki, T., 2003. CYP3A4 inducible model for in vitro analysis of human drug metabolism using a bioartificial liver. Hepatology 37, 665–673.

Kanto, T., Hayashi, N., Takehara, T., Hagiwara, H., Mita, E., Naito, M., Kasahara, A., Fusamoto, H., Kamada, T., 1994. Buoyant density of hepatitis C virus recovered from infected hosts: two different features in sucrose equilibrium density-gradient centrifugation related to degree of liver inflammation. Hepatology 19, 296–302.

Kawada, M., Nagamori, S., Aizaki, H., Fukaya, K., Niiya, M., Matsuura, T., Sujino, H., Hasumura, S., Yashida, H., Mizutani, S., Ikenaga, H., 1998. Massive culture of human liver cancer cells in a newly developed radial flow bioreactor system: ultrafine structure of functionally enhanced hepatocarcinoma cell lines. In Vitro Cell Dev. Biol. Anim. 34, 109–115.

Kuo, G., Choo, Q.L., Alter, H.J., Gitnick, G.L., Redeker, A.G., Purcell, R.H., Miyamura, T., Dienstag, J.L., Alter, M.J., Stevens, C.E., et al., 1989. An assay for circulating antibodies to a major etiologic virus of human non-A, non-B hepatitis. Science 244, 362–364.

Lanford, R.E., Guerra, B., Lee, H., Averett, D.R., Pfeiffer, B., Chavez, D., Notvall, L., Bigger, C., 2003. Antiviral effect and virus-host interactions in response to alpha interferon, gamma interferon, poly(i)–poly(c), tumor necrosis factor alpha, and ribavirin in hepatitis C virus subgenomic replicons. J. Virol. 77, 1092–1104.

Layden, T.J., Layden, J.E., Ribeiro, R.M., Perelson, A.S., 2003. Mathematical modeling of viral kinetics: a tool to understand and optimize therapy. Clin. Liver Dis. 7, 163–178.

Layden-Almer, J.E., Cotler, S.J., Layden, T.J., 2006. Viral kinetics in the treatment of chronic hepatitis C. J. Viral Hepat. 13, 499–504.

Lindenbach, B.D., Evans, M.J., Syder, A.J., Wolk, B., Tellinghuisen, T.L., Liu, C.C., Maruyama, T., Hynes, R.O., Burton, D.R., McKeating, J.A., Rice, C.M., 2005. Complete replication of hepatitis C virus in cell culture. Science 309, 623–626.

Lohmann, V., Korner, F., Koch, J., Herian, U., Theilmann, L., Bartenschlager, R., 1999. Replication of subgenomic hepatitis C virus RNAs in a hepatoma cell line. Science 285, 110–113.

Martell, M., Esteban, J.I., Quer, J., Genesca, J., Weiner, A., Esteban, R., Guardia, J., Gomez, J., 1992. Hepatitis C virus (HCV) circulates as a population of different but closely related genomes: quasispecies nature of HCV genome distribution. J. Virol. 66, 3225–3229.

Murakami, K., Ishii, K., Ishihara, Y., Yoshizaki, S., Tanaka, K., Gotoh, Y., Aizaki, H., Kohara, M., Yoshioka, H., Mori, Y., Manabe, N., Shoji, I., Sata, T., Bartenschlager, R., Matsuura, Y., Miyamura, T., Suzuki, T., 2006. Production of infectious hepatitis C virus particles in three-dimensional cultures of the cell line carrying the genome-length dicistronic viral RNA of genotype 1b. Virology 351, 381–392.

Pawlotsky, J.M., 2006. Hepatitis C virus population dynamics during infection. Curr. Top. Microbiol. Immunol. 299, 261–284.

Perelson, A.S., Herrmann, E., Micol, F., Zeuzem, S., 2005. New kinetic models for the hepatitis C virus. Hepatology 42, 749–754.

Poynard, T., Yuen, M.F., Ratziu, V., Lai, C.L., 2003. Viral hepatitis C. Lancet 362, 2095–2100.

Saito, I., Miyamura, T., Ohbayashi, A., Harada, H., Katayama, T., Kikuchi, S., Watanabe, Y., Koi, S., Onji, M., Ohta, Y., et al., 1990. Hepatitis C virus infection is associated with the development of hepatocellular carcinoma. Proc. Natl. Acad. Sci. U.S.A. 87, 6547–6549.

Shimizu, Y.K., Hijikata, M., Iwamoto, A., Alter, H.J., Purcell, R.H., Yoshikura, H., 1994. Neutralizing antibodies against hepatitis C virus and the emergence of neutralization escape mutant viruses. J. Virol. 68, 1494–1500.

Suzuki, T., Omata, K., Satoh, T., Miyasaka, T., Arai, C., Maeda, M., Matsuno, T., Miyamura, T., 2005. Quantitative detection of hepatitis C virus (HCV) RNA in saliva and gingival crevicular fluid of HCV-infected patients. J. Clin. Microbiol. 43, 4413–4417.

Tagawa, M., Kato, N., Yokosuka, O., Ishikawa, T., Ohto, M., Omata, M., 1995. Infection of human hepatocyte cell lines with hepatitis C virus in vitro. J. Gastroenterol. Hepatol. 10, 523–527.

Wakita, T., Pietschmann, T., Kato, T., Date, T., Miyamoto, M., Zhao, Z., Murthy, K., Habermann, A., Krausslich, H.G., Mizokami, M., Bartenschlager, R., Liang, T.J., 2005. Production of infectious hepatitis C virus in tissue culture from a cloned viral genome. Nat. Med. 11, 791–796.

Zhong, J., Gastaminza, P., Cheng, G., Kapadia, S., Kato, T., Burton, D.R., Wieland, S.F., Uprichard, S.L., Wakita, T., Chisari, F.V., 2005. Robust hepatitis C virus infection in vitro. Proc. Natl. Acad. Sci. U.S.A. 102, 9294–9299.

東医大誌 66(2): 212-223, 2008

ヒト肝癌細胞の三次元培養化に伴う遺伝子発現変動の網羅的解析

葛岡 健太郎[1)] 岩田 耕一郎[2)3)] 吉崎 佐矢香[3)]
相崎 英樹[3)] 鈴木 哲朗[3)] 長尾 桓[1)]

[1)]東京医科大学外科学第五講座
[2)]東京薬科大学薬学部医療薬学科臨床薬理学
[3)]国立感染症研究所ウイルス第二部

【要旨】 肝由来細胞の単層培養系は細胞極性など肝組織本来の特性が失われている。ヒト肝癌細胞株を立体的に培養し本来の形態に近似させることで、単層培養系に比べてどのような遺伝子の発現が変化するかを解析するため、ハイドロゲル TGP を利用した HepG2 細胞の三次元培養系を確立した。TGP 中では細胞増殖速度は低下するものの立体的なスフェロイド構造が形成されることを見出し、マイクロアレイ解析の結果、三次元培養に伴い細胞増殖制御、細胞分化調節、細胞内輸送、脂質代謝に関連する遺伝子群の発現変動が認められた。その中で、IGFBP3 の発現上昇は特に顕著であり、IGFBP3 を強制発現させた HepG2 細胞では増殖効率の低下が認められたことから、肝癌細胞の三次元培養化に伴う IGFBP3 の発現上昇が細胞増殖度低下に寄与している可能性が示唆された。さらに IGFBP3 発現によって誘導される遺伝子群も同定しており、以上の結果は、肝癌細胞の増殖能、肝組織の生物学的特性発現の分子機構を解析する上で有用な知見となる。

はじめに

臓器、組織を形成する多くの細胞は通常の単層培養実験系では細胞極性など本来の生物学的性質が失われている。これらの細胞は、立体的に三次元培養することにより細胞内分子群が秩序正しく空間的に配置され極性を有し、また細胞間ジャンクション構造を形成するようになることが知られている[1)]。細胞の極性は細胞機能発現の基盤となるものと考えられているが、このような形態変化がどのような分子メカニズムで細胞機能を制御しているかは明らかにされていない。本研究では、低温 (15℃以下) で水溶液、高温 (25℃以上) でゲル状となる[2)3)] 温度感受性ハイドロゲル Thermo-reversible Gelation Polymer (TGP) を用いて、ヒト肝癌細胞株の中で細胞生物学研究に最も広く用いられているヒト肝癌細胞株 HepG2 の三次元培養系の樹立を試み、スフェロイド形成に伴う細胞の遺伝子発現変化をマイクロアレイ法で網羅的に解析した。

マイクロアレイ解析により三次元培養系で発現が有意に亢進した遺伝子群の中で細胞増殖制御に関与する Insulin-like growth factor binding protein 3 (IGFBP3) に注目した。IGFBP3 は Insulin-like growth factor (IGF) と結合しその作用を調節すること、細胞増殖を負に制御しうることが知られている。培養系による発現レベルの違いを定量 RT-PCR 法及びウエスタンブロット法で解析した。さらに、本研究で観察された IGFBP3 の発現変化が HepG2 細胞の増殖能に影響を与えるかを調べるため、HepG2 細胞に IGFBP3 を強制発現させることによって細胞の増殖効率に変化が見られるかを解析した。

方法・材料

1. TGP を用いた細胞培養

ヒト肝細胞癌由来細胞株 HepG2 は 10% ウシ胎児血

2007 年 11 月 2 日受付、2007 年 12 月 4 日受理
キーワード: HepG2、IGFBP3、三次元培養、TGP
(別冊請求先: 〒 192-0042 東京都八王子市中野山王 2-15-16 八王子山王病院 葛岡健太郎)

清添加 Dulbecco's modified Eagle's medium (DMEM) (和光純薬工業、Osaka, Japan) を培地として用い、5% CO_2 存在下、37℃で培養した。固形化 TGP (Mebiol Gel MB-10；Mebiol, Tokyo, Japan) に上記培地を 10 ml 加えて 4℃で 7 日間静置し完全にゾル化した後使用した。このゾル化 TGP 1.8 ml に細胞 6×10^6 cells/ml を 0.2 ml 加え細胞懸濁ゾルを調製した。この調製は氷上で行った。細胞懸濁ゾル 0.6 ml を 35 mmϕ ディッシュ (Sumitomo Bakelite, Tokyo, Japan) に分注し 37℃でゲル化させた。さらに 37℃に加温した培地 3 ml を重層し培養を開始した。細胞を回収する場合は、培養ディッシュを 4℃で冷却し TGP をゾル化させた後、4 倍量の培地で希釈し遠心操作により細胞を沈殿させた。対照試料とする単層培養は 100 mmϕ ディッシュに 1.2×10^6 cells の細胞を播種して培養した。

2. DNA マイクロアレイ解析

DNA チップは Human genome Focus Array (Affymetrix, Tokyo, Japan) を用いた。このアレイには NCBI RefSeq データベース由来の約 8,973 遺伝子が搭載されている。測定データの解析には AFFYMETRIX GeneChip Operating Software 1.0 (http://www.affymetrix.com/jp/products/software/specific/gcos.affx) を用い、各遺伝子についての発現の有無を Absolute analysis で、サンプル間での発現量の比較を Comparison analysis によって行った。

3. RNA の調製

細胞の total RNA の調製には TRIZOL® Reagent (Invitrogen, Tokyo, Japan) を使用した。TGP 培養後、15 ml チューブに回収した細胞は、PBS で 1 回洗浄した後、400 μl の TRIZOL® Reagent に溶解させ、1.5 ml チューブに回収した。5 分間室温で静置した後、200 μl のクロロホルムを加え、30 秒攪拌し、5 分間氷上に置いた。12,000 rpm、15 分間遠心し、水層を回収しイソプロパノール 400 μl を加えた。室温で 10 分間放置した後、上記のように遠心操作を行いペレットに 800 μl の 75% エタノールを加え沈殿させた。

4. 定量 RT-PCR 解析

IGFBP3, N-myc (NDRG1), Solute e carrier family 26, member3 (SLC26A3), FXYD domain containing ion transport regulator 1 (phospholemman) (FXYD1), Ceruloplasmin (CP), Cholinergic receptor, nicotinic, beta polypeptide 1 (CHRNB1), Tensin (TNS) 遺伝子の PCR プライマー及び蛍光標識プローブはそれぞれ Applied Biosystems (Foster, CA, USA) より購入した。ワンステップ RT-PCR 反応には、TaqMan™ one-step PCR master mix reagents kit (Applied Biosystems) を用いた。48℃で 30 分間、逆転写反応を行い、95℃、10 分間処理した後、PCR 反応として 95℃：15 秒、60℃：1 分を 60 サイクル行った。一連の反応及び増幅 cDNA の検出には ABI PRISM 7700 TaqMan™ sequence detector (Applied Biosystems) を用いた。

5. 統計学的解析

mRNA 発現量の統計学的有意差は Mann-Whitney U-test によって検定した。統計解析には統計ソフトウェア StatView 5.0 (SAS Institute Inc, Cary, NC) を用いた。

6. ウエスタンブロッティング

細胞蛋白質の抽出には Passive Lysis Buffer (Promega, Tokyo, Japan) を用い、超音波細胞破砕装置 BIORUPTOR (Toshodenki, Tokyo, Japan) で細胞破壊操作を行った。遠心後の上清について BCA™ Protein assay kit (Pierce, Rockford, IL) を用いて蛋白濃度を測定し、一定量ずつ SDS-ポリアクリルアミドゲル電気泳動を行った。メンブレンへのブロッティングには Trans-Blot SD (Bio-Rad, Richmond, CA) を用い、4% スキムミルク (Morinaga, Tokyo, Japan) でブロッキングを行った。500 倍希釈した抗 IGFBP-3 抗体 (Upstate Inc, Lake Placid, NY) を 37℃、1 時間反応させた後、TTBS 溶液 (20 mM Tris-HCl, 0.5 M NaCl, 0.05% Tween 20)で 3 回洗浄した。3,000 倍希釈の抗ウサギ IgG 抗体 (Cell Signaling Technology, Danvers, MA) を 37℃、1 時間反応させた後、TTBS 溶液にて洗浄し、Super Signal® West Pico Chemiluminescent Substrate (Pierce) を用いて発色させた。内部コントロールとして GAPDH の発現を同様に解析した。

7. IGFBP3 遺伝子の細胞への導入

IGFBP3 発現プラスミド pSF398 は Dr. Sue M. Firth (Kolling Institute of Medical, University of Sydney, Australia) より供与された。HepG2 細胞を K-PBS (30 mM NaCl, 120 mM KCl, 8 mM Na_2HPO_4, 1.5 mM KM_2PO_4, 5 mM $MgCl_2$) で洗浄し細胞懸濁液を加えた。Gene Pulser Cuvette (Bio-Rad) に移し、pSF398 を添加し氷上に 5 分間静置した。GENE PULSER (Bio-Rad) にセットし 975 μFD、300 V でエレクトロポレーションを行った。100 mmϕ ディッシュに細胞を播種し一晩培養後、トリプシンで細胞を剝がし、細胞数をカウントし、12-well plate (Iwaki, Tokyo, Japan)

に分注し、その後 1, 2, 3, 4, 5, 6 日目に細胞数をカウントした。培地は 4 日目に交換した。

8. IGFBP3 発現に伴って変化する遺伝子発現の網羅的解析

上記 7. で遺伝子導入を行った HepG2 細胞を 100 mmϕ ディッシュに捲き戻し、1 日目と 3 日目に培地交換を行い、4 日目に細胞を回収した。前述のマイクロアレイと同様の方法により IGFBP3 発現に伴う遺伝子発現の一斉解析を行った。

結　果

1. TGP を用いた HepG2 細胞の三次元培養

Single cell に分散した HepG2 をゾル化 TGP に懸濁した後、37℃でゲル化した (TGP 培養)。細胞の増殖度、形態を通常の単層培養系と比較した結果を Fig. 1 に示した。TGP 培養は、単層培養に比べ緩やかではあるがコンスタントな細胞増殖が認められた (Fig. 1A)。Doubling time は TGP 培養では、約 48 時間、単層培養では約 38 時間であり、培養 7 日後の細胞数は単層培養の約 1/3 であった。位相差顕微鏡での細胞形態観察の結果を Fig. 1B に示した。単層培養では、扁平状の形態を示したのに対し、TGP 内で増殖した HepG2 細胞は球形状の細胞塊 (スフェロイド) 形成が観察された。培養 7 日目では、TGP 内で直径約 50 μm 程度のスフェロイド形成が認められた。このように細胞増殖度は単層培養より低いものの TGP 内に HepG2 細胞が三次元培養化できることが明らかとなった。

2. マイクロアレイ解析による遺伝子発現プロファイリングの比較

HepG2 細胞の三次元培養化に伴う遺伝子の発現変化を網羅的に解析するためマイクロアレイ解析を行った。測定した 8,973 種類の遺伝子のうち、4,941 種類 (56%) の遺伝子が比較可能であった。87 種類 (1%) の遺伝子は単層培養系に比べ三次元培養系で発現レベルが 2 倍以上に上昇していた。この中には細胞増殖、分化の制御に関連する遺伝子が IGFBP3 など 5 種類、輸送に関係する遺伝子が SLC26A3 など 10 種類、代謝に関連する遺伝子が Tyrosinase-related protein 1 (TYRP1) など 38 種類、免疫応答に関係する遺伝子が CD9 antigen (CD9) など 4 種類、シグナル伝達に関係する遺伝子が Troponin C, slow (TNNC1) など 17 種類、アポトーシスに関係する遺伝子が BCL2/adenovirus E1B 19kDa interacting protein 3 (BNIP3L) など 5 種類含まれていた (Table 1)。一方、20 種類 (0.2%) の遺伝子が三次元培養系で発現レベルが 1/2 以下まで低下していた。その中には増殖、分化を制御する遺伝子が Insulin growth factor 1 (IGF1) など 3 種類、代謝に関係する遺伝子が Primase polypeptide 2A (PRIM2A) など 9 種類、シグナル伝達に関係する遺伝子が Guanine nucleotide binding protein (G protein), gamma 13 (GNG13) など 6 種類含まれていた (Table 2)。

3. 遺伝子発現変化の mRNA 定量的解析

マイクロアレイ解析で単層培養系に比べ三次元培養系で発現上昇が認められた遺伝子群のうち、増殖調節に関係する IGFBP3、NDRG1、細胞内物質移動に関

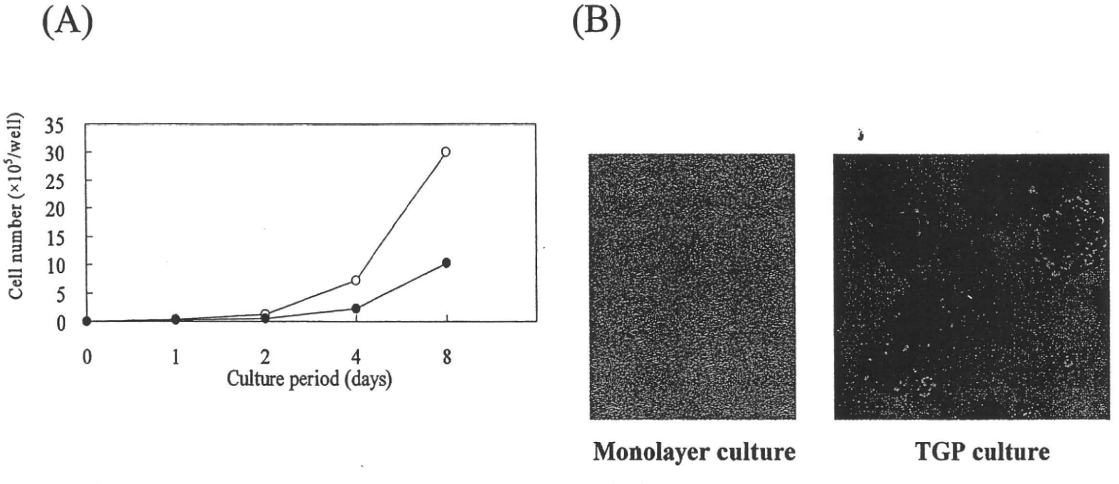

Fig. 1 Establishment of the three-dimensional culture of HepG2 cells in TGP.
(A) Cell growth curves. (B) Morphological comparison of the cells with monolayer culture (left) and with TGP culture (right).

Table 1 Genes with increased levels of expression in the TGP culture.

SLR	Genbank ID	Common name	Gene name
			Cell growth, differentiation
2.9	NM 003116.1	SPAG4	sperm associated antigen 4
1.7	NM 030773	TUBB1	tubulin, beta 1
1.2	NM 006576	AVIL	advillin
1	NM 002593	PCOLCE	procollagen C-endopeptidase enhancer
1	NM 013332.1	HIG2	hypoxia-inducible protein 2
			Apoptosis
2.5	M31159	IGFBP3	insulin-like growth factor binding protein 3
2.4	NM 006096	NDRG1	N-myc downstream regulated gene 1
2	U15172	BNIP3L	BCL2/adenovirus E1B 19 kDa interacting protein 3-like
1.2	NM 004052	BNIP3	BCL2/adenovirus E1B 19 kDa interacting protein 3
1	NM 003810	TNFSF10	tumor necrosis factor (ligand) superfamily, member 10
			Transport
4.4	NM 002635	SLC26A3	solute carrier family 26, member 3
2.9	NM 005031	FXYD1	FXYD domain containing ion transport regulator 1 (phospholemman)
1.9	NM 000040	APOC3	apolipoprotein C-III
1.7	AF162690	TTR	transthyretin (prealbumin, amyloidosis type I)
1.4	NM 001122.2	ADFP	adipose differentiation-related protein
1.3	NM 030971	BA108L7.2	similar to rat tricarboxylate carrier-like protein
1.1	NM 003046	SLC7A2	solute carrier family 7 (cationic amino acid transporter, y+ system), member 2
1.1	NM 001311.3	CRIP1	cysteine-rich protein 1 (intestinal)
1.1	AF067864	TFR2	transferrin receptor 2
1	NM 005835	SLC17A2	solute carrier family 17 (sodium phosphate), member 2
			Metabolism
4	NM 000550	TYRP1	tyrosinase-related protein 1
2.6	NM 001216	CA9	carbonic anhydrase IX
2.4	NM 000096	CP	ceruloplasmin (ferroxidase)
2.3	NM 201555.1	FHL2	four and a half LIM domains 2
2.3	NM 000045	ARG1	arginase, liver
2.1	NM 004566	PFKFB3	6-phosphofructo-2-kinase/fructose-2,6-biphosphatase 3
2.1	NM 002591	PCK1	phosphoenolpyruvate carboxykinase 1 (soluble)
1.9	NM 001443	FABP1	fatty acid binding protein 1, liver
1.8	NM 001124	ADM	adrenomedullin
1.8	NM 003670	BHLHB2	basic helix-loop-helix domain containing, class B, 2
1.8	NM 001674	ATF3	activating transcription factor 3
1.8	NM 021603	FXYD2	FXYD domain containing ion transport regulator 2
1.8	NM 000602.1	SERPINE1	serpin peptidase inhibitor
1.7	NM 000158.1	GBE1	glucan (1, 4-alpha-), branching enzyme 1
1.6	NM 012331	MSRA	methionine sulfoxide reductase A
1.6	NM 002108	HAL	histidine ammonia-lyase
1.5	NM 016236	AGXT	alanine-glyoxylate aminotransferase
1.5	AF116713	ITIH1	inter-alpha (globulin) inhibitor H1
1.5	NM 012228.2	MSRB	methionine sulfoxide reductase B2
1.5	NM 002217.2	ITIH3	inter-alpha (globulin) inhibitor H3
1.4	NM 031244	SIRT5	sirtuin (silent mating type information regulation 2 homolog) 5 (S. cerevisiae)
1.4	NM 001801.2	CDO1	cysteine dioxygenase
1.3	NM 015869	PPARG	peroxisome proliferative activated receptor, gamma
1.3	NM 002610	PDK1	pyruvate dehydrogenase kinase, isoenzyme 1
1.3	NM 005165.2	ALDOC	aldolase C
1.2	NM 002084	GPX3	glutathione peroxidase 3 (plasma)

Table 1 Continued.

SLR	Genbank ID	Common name	Gene name
1.2	X86401	GATM	glycine amidinotransferase (L-arginine : glycine amidinotransferase)
1.2	NM 001360	DHCR7	7-dehydrocholesterol reductase
1.1	NM 002773.2	PRSS8	protease
1.1	NM 003528.2	HIST2H2BE	histone cluster 2
1	NM 001916	CYC1	cytochrome c-1
1	AI189359	MVD	mevalonate (diphospho) decarboxylase
1	NM 001461	FMO5	flavin containing monooxygenase 5
1	NM 005962	MXI1	MAX interactor 1
1	AI313324	HIST2H2AA	histone 2, H2aa
1	NM 003212	TDGF1	teratocarcinoma-derived growth factor 1
1	NM 005398.3	PPP1R3C	protein phosphatase 1
1	NM 000504.3	F10	coagulation factor X
			Immune response
1.9	NM 014257	CD209L	CD209 antigen-like serine proteinase inhibitor, class E
1.7	NM 001769	CD9	CD9 antigen (p24)
1.3	BG327863	CD24	CD24 antigen (small cell lung carcinoma cluster 4 antigen)
1.1	NM 003734	AOC3	amine oxidase, copper containing 3 (vascular adhesion protein 1)
			Signal transduction
4.4	AF020769	TNNC1	troponin C, slow
2.4	NM 018274	TNS	tensin
2.1	NM 000747	CHRNB1	cholinergic receptor, nicotinic, beta polypeptide 1 (muscle)
1.9	NM 015385	SORBS1	sorbin and SH3 domain containing 1
1.6	NM 000211	ITGB2	integrin, beta 2 (antigen CD18 (p95), macrophage antigen 1 (mac-1) beta subunit)
1.5	M13981	INHA	inhibin, alpha
1.4	NM 002842	PTPRH	protein tyrosine phosphatase, receptor type, H
1.3	AF084462	RIT1	Ras-like without CAAX 1
1.3	NM 004417	DUSP1	dual specificity phosphatase 1
1.2	AF022375	VEGF	vascular endothelial growth factor
1.2	NM 006183	NTS	neurotensin
1.1	AI690165	RAB26	RAB26, member RAS oncogene family
1.1	AL136139	NEDD9	neural precursor cell expressed, developmentally down-regulated 9
1	NM 002205	ITGA5	integrin, alpha 5 (fibronectin receptor, alpha polypeptide)
1	BC000658	STC2	stanniocalcin 2
1	NM 000799	EPO	erythropoietin
1	NM 001321	CSRP2	cysteine and glycine-rich protein 2
1	L22431	VLDLR	very low density lipoprotein receptor

わるSLC26A3、FXYD1、CP、CHRNB1、信号伝達に関わるTNSについて、両培養細胞中でのmRNA発現をreal-time RT-PCR法により定量的に解析した。アクチンmRNAの発現量を各培養系の内部標準とした。その結果、三次元培養系におけるIGFBP3の発現が単層培養に比べ約4倍亢進していることが示された (Fig. 2A)。IGFBP3以外の遺伝子については必ずしも有意な差は認められなかった。

4. 蛋白レベルでの遺伝子発現の比較

三次元培養化に伴う遺伝子発現変動のうちIGFBP3の発現上昇が顕著であることが示されたが、実際に蛋白質レベルでも培養系間で差異を認めるかをウエスタンブロット法で解析した。Fig. 2に示すように、単層培養した細胞に比べて三次元培養した細胞においてIGFBP3蛋白量が増加していることが示された。

5. IGFBP3強制発現に伴う細胞増殖能の変化

IGFBP3発現ベクター導入後6日目まで観察したところ、IGFBP3高発現細胞ではコントロール (empty vector導入) 細胞と比べ増殖速度の低下が認められた。Doubling timeはIGFBP3高発現細胞が約50時間であったのに対しコントロール細胞では約44時間であった (Fig. 3)。

IGFBP3発現に伴って変化する遺伝子発現の網羅的解析

三次元培養化に伴いIGFBP3の発現が上昇し、この発現変化が細胞の増殖効率の制御に関与する可能性が示唆されたが、HepG2細胞におけるIGFBP3による増殖制御の分子機構を明らかにしていくため、IGFBP3発現に伴って変化する遺伝子発現をマイクロアレイ法によって網羅的に解析した。IGFBP3の高発現に伴い0.5% (53種類) の遺伝子の発現レベルが2倍以上に上昇した (Table 3)。この中にはシグナル伝達

Table 2 Genes with decreased levels of expression in the TGP culture.

SLR	Genbank ID	Common name	Gene name
		Cell growth, differentiation, anti-apoptosis	
−2.4	NM 000618.2	IGF1	insulin-like growth factor 1 (somatomedin C)
−1	NM 005219.2	DIAPH1	diaphanous homolog 1 (Drosophila)
−1	NM 003246.2	THBS1	thrombospondin 1
		Metabolism	
−3.9	NM 000947	PRIM2A	primase, polypeptide 2A, 58 kDa
−3.1	NM 001644.3	APOBEC1	apolipoprotein B mRNA editing enzyme
−2.8	O75604-2	USP2	ubiquitin specific protease 2
−2.6	NM 015886.3	PI15	peptidase inhibitor 15
−2.6	NM 006919.1	SERPINB3	serpin peptidase inhibitor, clade B (ovalbumin), member 3
−2.6	NM 000153	GALC	galactosylceramidase (Krabbe disease)
1	NM 005575.2	LNPEP	carbonic anhydrase IX
−1	NM 000214.1	ID3	inhibitor of DNA binding 3, dominant negative helix-loop-helix protein
−1	NM 003538.3	HIST1H4A	histone cluster 1, H4a
		Transport	
−1.8	NM 003043.2	SLC6A6	solute carrier family 6 (neurotransmitter transporter, taurine), member 6
		Signal transduction	
−3	NM 016541	GNG13	guanine nucleotide binding protein (G protein), gamma 13
−2.5	NM 005242.3	F2RL1	coagulation factor II (thrombin) receptor-like 1
−2.1	NM 001050.2	SSTR2	somatostatin receptor 2
−1.3	NM 004843.2	IL27RA	interleukin 27 receptor, alpha
−1.1	NM 002760.3	PRKY	protein kinase, Y-linked
−1	NM 000214.1	JAG1	jagged 1 (Alagille syndrome)
		Immune response	
−3.9	NM 001562.2	IL18	interleukin 18

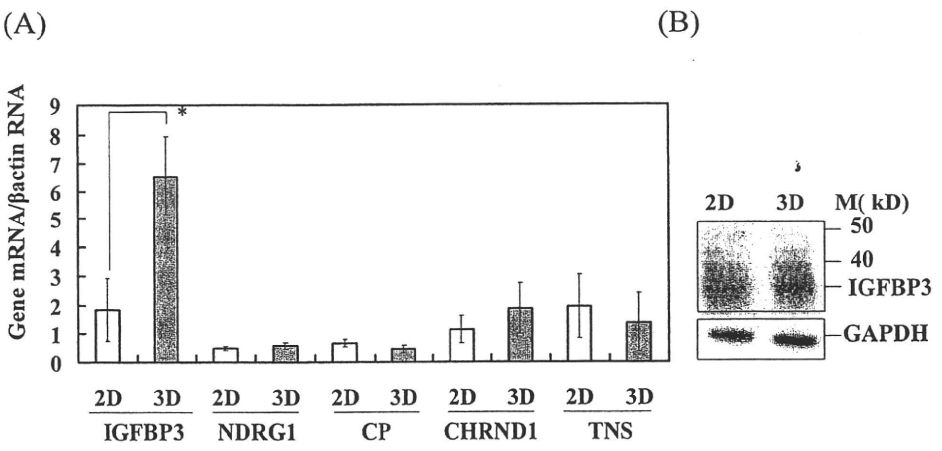

Fig. 2 IGFBP3 is highly expressed in the TGP culture in comparison with the monolayer culture.
(A) Real-time RT-PCR analysis. Average values of three independent measurements with standard deviations are shown. There is a significant difference between IGFBP3 expression in the monolayer (2D) culture and that in the TGP (3D) culture (*: $p<0.05$; student's t test). (B) Western blot analysis. Cell lysates from 2D and 3D cultures were resolved on a SDS-polyacrylamide gel, followed by probing with anti-IGFBP3 or anti-GAPDH antibody.

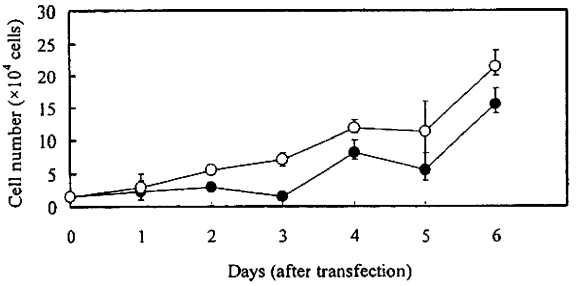

Fig. 3 Cell growth curves of HepG2 cells with or without over-expression of IGFBP3.
Cells were transfected with IGFBP3-expression plasmid (closed circle) or with an empty vector (open circle). Results show the mean cell numbers in three dishes with standard deviation.

に関係する遺伝子が Protein kinase, cGMP-dependent, type II (PRKG2) など16種類、核酸代謝に関連する遺伝子が Forkhead box D2 (FOXD2) など12種類、増殖、分化の制御に関連する遺伝子が Cadherin 11, type 2, OB-cadherin (CDH11) など7種類、輸送に関係する遺伝子が Cyclic nucleotide gated channel alpha 3 (CNGA3) など5種類、細胞骨格、形態形成に関係する遺伝子が1種類含まれていた。一方、0.5% (41種類) の遺伝子の発現レベルが IGFBP3 の高発現によって逆に 1/2 以下まで低下していた。その中にはシグナル伝達に関係する遺伝子が HCF-binding transcription factor Zhangfei (ZF) など14種類、核酸代謝に関連す

Table 3 Genes with increased levels of expression in the IGFBP3-overexpressing cells.

SLR	Genbank ID	Common name	Gene name
			Cell growth, differentiation, apoptosis
4.4	NM 001797	CDH11	cadherin 11, type 2, OB-cadherin (osteoblast)
1.9	AK000947	MYH7B	myosin, heavy polypeptide 7B, cardiac muscle, beta
1.7	NM 004543	NEB	nebulin
1.7	NM 003803	MYOM1	myomesin 1 (skelemin) 185 kDa
1.5	NM 006771	KRT38	keratin 38
1.4	NM 000231	SGCG	sarcoglycan, gamma (35kDa dystrophin-associated glycoprotein)
1.1	NM 000259	MYO5A	myosin VA (heavy polypeptide 12, myoxin)
			Transport
3.2	NM 001298	CNGA3	cyclic nucleotide gated channel alpha 3
1.9	AF155159	AP4S1	adaptor-related protein complex 4, sigma 1 subunit
1.5	NM 004732	KCNAB3	potassium voltage-gated channel, shaker-related subfamily, beta member 3
1.4	U27699	SLC6A12	solute carrier family 6 member 12
1.2	NM 001891	CSN2	casein beta
			Metabolism
1.5	NM 000764	CYP2A6	cytochrome P450, family 2, subfamily A, polypeptide 6
1.0	AI685944	IAPP	islet amyloid polypeptide
			Cell structure
1.3	NM 004434	EML1	echinoderm microtubule associated protein like 1
			Signal transduction
5.0	NM 006259	PRKG2	protein kinase, cGMP-dependent, type II
4.4	NM 007368	RASA3	RAS p21 protein activator 3
4.0	NM 030901	OR7A17	olfactory receptor, family 7, subfamily A, member 17
3.7	NM 003914	CCNA1	cyclin A1
3.5	NM 017412	FZD3	frizzled homolog 3 (Drosophila)
2.7	NM 002649	PIK3CG	phosphoinositide-3-kinase, catalytic, gamma polypeptide
2.7	Z81148	GNRHR	gonadotropin-releasing hormone receptor
2.2	NM 000805	GAST	gastrin
2.1	NM 000965	RARB	retinoic acid receptor, beta
2.0	NM 005739	RASGRP1	RAS guanyl releasing protein 1 (calcium and DAG-regulated)
1.9	NM 005761	PLXNC1	plexin C1
1.9	NM 021920	SCT	secretin
1.6	NM 005044	PRKX	protein kinase, X-linked
1.6	NM 005621	S100A12	S100 calcium binding protein A12 (calgranulin C)
1.3	D10537	MPZ	myelin protein zero (Charcot-Marie-Tooth neuropathy 1B)
1.2	NM 018971	GPR27	G protein-coupled receptor 27

Table 3 Continued.

SLR	Genbank ID	Common name	Gene name
			Regulation of nucleobase
4.4	NM 004474	FOXD2	forkhead box D2
3.9	AV727449	PCAF	p300/CBP-associated factor
3.6	NM 003433	ZNF132	zinc finger protein 132
3.6	AA166895	NHLH2	nescient helix loop helix 2
3.2	U64315	ERCC4	excision repair cross-complementing rodent repair deficiency
2.2	NM 022898	BCL11B	B-cell CLL/lymphoma 11B (zinc finger protein)
1.7	AA488672	KLF7	kruppel-like factor 7 (ubiquitous)
1.4	N91520	ZNF202	zinc finger protein 202
1.3	NM 005066	SFPQ	splicing factor proline/glutamine-rich
1.3	NM 005419	STAT2	signal transducer and activator of transcription 2, 113 kDa
1.2	NM 004852	ONECUT2	one cut domain, family member 2
1.1	X55005	THRA	thyroid hormone receptor, alpha
			Others or unknown
2.5	NM 001036	RYR3	ryanodine receptor 3
2.4	AF250321	C3orf28	chromsome 3 open reading frame 28
2.3	AW299958	PAPSS2	3′-phosphoadenosine 5′-phosphosulfate synthase 2
2.3	NM 004791	ITGBL1	integrin, beta-like 1 (with EGF-like repeat domains)
2.2	NM 014332	SMPX	small muscle protein, X-linked
1.6	NM 021123	GAGE7	G antigen 7
1.6	NM 021570	BARX1	BarH-like homeobox 1
1.2	BF508685	CTRL	chymotrypsin-like
1.1	NM 004960	FUS	fusion (involved in t (12 ; 16) in malignant liposarcoma)
1.1	NM 017503	SURF2	surfeit 2

る遺伝子がBasic helix-loop-helix domain containing, class B, 2 (BHLHB2) など7種類、増殖、分化を制御する遺伝子が6種類含まれていた (Table 4)。

考　　察

ヒト肝癌細胞株を立体的に培養し、細胞本来の形態に近い状態を保つことで、一般的な単層培養系とどのような遺伝子の発現が異なるかを解析するため、TGPを利用したHepG2細胞の三次元培養系を確立した。本研究グループでは、すでにヒト肝癌細胞株Huh-7のTGP培養系を作製し、これが肝炎ウイルスの増殖、粒子産生モデルとして有用であることを示している[4]。Huh-7細胞をTGP培養した場合、単層培養に比べ細胞増殖度の低下が観察されているが、今回、HepG2細胞の場合も同様の傾向が認められた。

村上らは、TGPで三次元培養したHuh7由来細胞株(RCYM1)の微細構造を透過型及び走査型電子顕微鏡で観察し、単層培養に比べて細胞表面の微絨毛がよく発達し、また微小胆管様の構造が細胞間に認められることを報告している[4]。今回、HepG2細胞をTGPで7日間培養することにより直径約50 μm程度のスフェロイド構造が形成されることを見出したが、この細胞塊の切片を作製し電子顕微鏡観察を行ったところ、同様の構造を認め、また細胞間接着面にジャンクション構造が観察された (吉崎ら投稿準備中)。これらの特徴は、人工肝臓モデルであるラジアルフロー型バイオリアクターで培養された高分化型ヒト肝癌細胞で認められる特徴と一致しており[5-7]、株化癌細胞株であっても、三次元培養化に伴って生態の肝臓組織に近い形態をとりうることを示している。TGPは、温度感受性のポリマー素材を使用したマトリックスで、寒天ゲルやゼラチンゲルとは逆に低温 (15℃以下) で水溶液、高温 (25℃以上) でゲル状となる。ゲルの硬さを細胞、組織が自由に生育できる範囲に設定しているため、細胞等の立体的な培養が可能である。また、温度を下げることにより、容易に融解するため、細胞へのダメージを最小限にとどめた形で回収することができる。また培養に用いる器具は、通常の細胞培養用のものであり特殊な装置を必要としない。人工肝臓装置などと比べ汎用性に優れ多様な用途に利用することが可能である。

細胞の三次元培養化に伴う遺伝子の発現変化を網

Table 4 Genes with decreased levels of expression in the IGFBP3-overexpressing cells.

SLR	Genbank ID	Common name	Gene name
		Cell growth, differentiation, apoptosis	
-3.4	NM 021127	PMAIP1	phorbol-12-myristate-13-acetate-induced protein 1
-3.4	NM 015888	HOOK1	hook homolog 1 (Drosophila)
-1.1	X15132	SOD2	superoxide dismutase 2, mitochondrial
-1.0	NM 001706	BCL6	B-cell CLL/lymphoma 6 (zinc finger protein 51)
-1.0	M92934	CTGF	connective tissue growth factor
-1.0	NM 013332	HIG2	hypoxia-inducible protein 2
		Metabolism	
-1.8	NM 000188	HK1	hexokinase 1
		Signal transduction	
-3.5	NM 021212	ZF	HCF-binding transcription factor Zhangfei
-2.3	AW189015	EFNA3	ephrin-A3
-2.3	BC002836	EFCAB2	EF-hand calcium binding domain 2
-2.1	NM 001554	CYR61	cysteine-rich, angiogenic inducer, 61
-1.9	NM 004417	DUSP1	dual specificity phosphatase 1
-1.2	NM 002847	PTPRN2	protein tyrosine phosphatase, receptor type, N polypeptide 2
-1.2	BC003143	DUSP6	dual specificity phosphatase 6
-1.1	NM 006018	GPR109B	G protein-coupled receptor 109B
-1.1	NM 015675	GADD45B	growth arrest and DNA-damage-inducible, beta
-1.0	NM 006472	TXNIP	thioredoxin interacting protein
-1.0	BG546884	CRIM1	cysteine rich transmembrane BMP regulator 1 (chordin-like)
-1.0	AW194730	STK17A	serine/threonine kinase 17a (apoptosis-inducing)
-1.0	AB011110	RASA4///FLJ21767	RAS p21 protein activator 4 /// hypothetical protein FLJ21767
-1.0	NM 020651	PELI1	pellino homolog 1 (Drosophila)
		Regulation of nucleobase	
-1.6	NM 003670	BHLHB2	basic helix-loop-helix domain containing, class B, 2
-1.6	NM 003407	ZFP36	zinc finger protein 36, C3H type, homolog (mouse)
-1.3	AB017493	KLF6	kruppel-like factor 6
-1.2	AL021977	MAFF	v-maf musculoaponeurotic fibrosarcoma oncogene homolog F (avian)
-1.1	NM 002229	JUNB	jun B proto-oncogene
-1.1	NM 001674	ATF3	activating transcription factor 3
-1.0	NM 005384	NFIL3	nuclear factor, interleukin 3 regulated
		Others or unknown	
-2.5	AL049250	LOC440345	hypothetical protein LOC440345
-1.4	AL136653	C10orf10	chromosome 10 open reading frame 10
-1.3	NM 001124	ADM	adrenomedullin
-1.3	BG232034	ATP5C1	ATP synthase, H+ transporting, mitochondrial F1 complex, gamma polypeptide 1
-1.0	NM 002541	OGDH	oxoglutarate (alpha-ketoglutarate) dehydrogenase (lipoamide)

羅的に解析するためマイクロアレイ解析を行った。TGP培養系と単層培養系では細胞の増殖速度は異なるものの、培養開始3日目ではどちらの培養系とも対数増殖期にあることから、この時点の細胞で遺伝子発現比較を行うこととした。解析の結果、TGP培養系と単層培養系で発現レベルが2倍以上異なった遺伝子は全体の1.2%(107遺伝子)であり、このうちTGP培養系で発現が亢進した遺伝子が87種類、低下したものが20種類であった。発現の亢進した遺伝子群の中では、BNIP3Lなど細胞増殖のdown-regulationに関連する遺伝子、FXYD2といったイオンなどの輸送に係わる遺伝子、またTYRP1など代謝関連遺伝子が特徴的であった。発現の低下した遺伝子としてIGF1のような細胞増殖のup-regulation関連遺伝子が含まれていたことを考えあわせると、三次元培養化に伴う細胞遺伝子の発現変動が、細胞の増殖低下、分化誘導の方向に働く可能性が考えられる。培養系の違いによって発現レベルの差が認められた遺伝子のうち、増殖調

節に関係するIGFBP3、NDRG1、細胞内物質移動に関わるSLC26A3、FXYD1、CP、CHRNB1、信号伝達に関わるTNSについて、7日間TGP培養および単層培養を行ったHepG2細胞を用いて、real-time RT-PCR法によりmRNA発現を定量的に解析した。その結果、TGP培養におけるIGFBP3の発現亢進が最も顕著であることが示された。さらにウエスタンブロット解析により、IGFBP3は蛋白質レベルでもTGP培養系で発現量が増加していることを明らかにした。

IGFBP3は、IGFに特異的に結合している蛋白質の一種である。血中ではIGF及びacid-labile subunitとともに約150 kDの三量体として存在している。IGFBP3は6種類のIGFBPの中では血中濃度が高くIGFの作用を調節していると考えられている[8-10]。IGFはインスリン様効果に加え、細胞DNA合成の調節に関与しており肝癌細胞などの増殖を促進する。一方、その生物活性はIGFBP3との結合により減弱することが知られている[11-13]。肝癌細胞株にIGFBP3を添加することにより細胞増殖が抑制されること[14]、生体内においてIGFBP3の発現が肝癌の大きさ、組織型、被膜浸潤、門脈浸潤の有無に関係し、発現が弱い場合肝癌患者の生存率も低くなること[15][16]などが報告されている。IGFBP3の癌細胞増殖抑制能にはこのようなIGFとの結合を介した作用の他に、最近ではIGF非依存的機構が知られるようになり[17]、アポトーシス促進、血管新生抑制などの作用が報告されているものの、その作用機序は未だ十分には解明されていない[18-20]。

HepG2細胞の増殖効率にIGFBP3が関与しているかを調べるため、細胞にIGFBP3を強制発現させ増殖曲線を求めた。予想通り、IGFBP3高発現細胞では増殖率の低下を認めたことから、三次元培養化に伴うIGFBP3の発現上昇が細胞増殖度低下に寄与している可能性が示唆された。さらに、IGFBP3の発現誘導に伴う遺伝子発現の変化を網羅的に解析したところ、IGFBP3発現レベルの異なる二種類の培養系で発現レベルが2倍以上変化した遺伝子は全体の1%（94遺伝子）であった。IGFBP3強制発現細胞で発現が亢進していた遺伝子の中には、PRKG2など細胞間シグナル伝達に係わる遺伝子、FOXD2など核酸代謝関連遺伝子が、発現が抑制された遺伝子にはZFなどシグナル伝達に係わる遺伝子や細胞増殖に係わるphorbol-12-myristate-13-acetate-induced protein 1 (PMAIP1)などが含まれていた。この結果は、IGFBP3の発現亢進に伴う癌細胞の増殖能、特性の変化の分子機構を解析する上で有用な知見となることが期待される。

本研究で初めて、肝癌細胞の三次元化培養に伴ってIGFBP3の発現が上昇することが明らかとなった。IGFBP3の遺伝子発現を制御する因子についてはいくつか報告されており、発現を亢進するものとしてPTEN[21]、COX-2[22]、DeltaNp63alpha[23]、GH[24]が、抑制するものとしてPTH[17]が挙げられる。またHIF-1αはIGFBP3の発現に必要とされている[25]。しかしながら、TGP培養においてこれらの遺伝子の発現変化は必ずしも顕著ではないため、三次元培養によるIGFBP3発現誘導の引き金となる因子の同定は今後の検討課題である。

結　論

ヒト肝癌細胞株を、本来の形態に近い立体的な状態で培養することにより変動する遺伝子発現を解析するため、ハイドロゲルTGPを利用したHepG2細胞の三次元培養系を確立し以下の知見を得た。

1. TGP中では細胞増殖速度は低下するものの、7日間培養で直径約50 μm程度のスフェロイド構造が形成された。

2. マイクロアレイ解析の結果、三次元培養に伴う1) 細胞増殖制御、2) 細胞分化調節、3) 細胞内輸送、4) 脂質代謝に関連する遺伝子群の発現変動が特徴的であった。

3. 単層培養に比べTGP培養で顕著にmRNAレベルが亢進していたIGFBP3は、蛋白質レベルでもTGP培養で発現量が高いことを確認した。

4. IGFBP3を強制発現させたHepG2細胞では増殖効率の低下が認められた。以上の結果より、肝癌細胞の三次元培養化に伴うIGFBP3の発現上昇が細胞増殖度低下に寄与している可能性が示唆された。

謝　辞

稿を終えるにあたり、直接御指導頂きました国立感染症研究所ウイルス第二部の皆様に心より感謝の意を表します。

文　献

1) Talamini MA, Kappus B, Hubbard A : Repolarization of hepatocytes in culture. Hepatology **25**: 167-172, 1997
2) 吉岡　浩、森　有一：熱可逆性三次元培養担体「メ